nature medicine

Article

https://doi.org/10.1038/s41591-026-04212-0

A quantitative DOPA decarboxylase biomarker for diagnosis in Lewy body disorders

Received: 21 March 2025

Accepted: 7 January 2026

Published online: 16 February 2026

Check for updates

A list of authors and their affiliations appears at the end of the paper

Accurate diagnosis of dementia with Lewy bodies (DLB) remains challenging, with misdiagnosis potentially leading to harmful treatment decisions. DOPA decarboxylase (DDC) shows promise as a cerebrospinal fluid (CSF) biomarker for DLB and Parkinson's disease (PD), but quantitative assays are needed for its clinical implementation. Here we report on the development of two DDC immunoassays and the extensive clinical validation of DDC across three clinical cohorts (n = 740), one biologically defined cohort (n = 253), one cohort with detailed dopamine transporter imaging information (n = 102) and one autopsy-confirmed cohort (n = 78). CSF DDC levels were significantly higher in DLB and PD (up to 2.5-fold versus controls; 1.9-fold versus AD), showing area under the curve values > 0.9 for differential diagnosis. Elevated CSF DDC was linked to the presence, but not severity, of motor impairment. In autopsy-confirmed DLB, higher CSF DDC correlated with progressing α-synuclein pathology and immunohistochemistry in DLB and PD brain tissue revealed colocalization of DDC and α-synuclein in the substantia nigra. These findings underscore DDC's value to support DLB and PD diagnosis, paving the way for its clinical implementation using the here-presented developed immunoassays.

Lewy body disorders (LBDs) including DLB and PD are the second most common neurodegenerative diseases after Alzheimer's Disease (AD) in older people[1]. The pathological hallmark of LBDs is the abnormal aggregation of proteins, lipids and organelles into so-called Lewy bodies (LBs) and Lewy neurites (LNs). The main constituent of these structures is the misfolded form of alpha-synuclein (α-syn), the first biological anchor in recently suggested characterization systems[2,3]. LBs are present in different brain areas, in the brainstem and/or amygdala in early stages and later also in the neocortex. The exact cause of their formation as well as their role is still not fully understood. The loss of dopaminergic neurons in the substantia nigra[4], and related nigrostriatal dopaminergic dysfunction, is another pathological hallmark in LBDs[2,5]. In addition to the pathological similarities, LBDs also share some clinical features, such as motor signs of bradykinesia and rigidity. While PD is mainly characterized by impaired motor functioning[6], DLB core features additionally include fluctuations of cognition, visual hallucinations and rapid eye movement REM sleep behavior disorder (RBD)[7], and cognitive impairment/dementia is an overlapping feature with AD. Due to the wide pathological and clinical overlap with AD and the heterogeneous clinical manifestation, an accurate diagnosis of DLB is still challenging[8]. This hampers prediction of the disease course and patient stratification for clinical trials, and can lead to inappropriate treatment approaches with harmful effects on the patients, highlighting the need for disease-specific biomarkers to facilitate DLB diagnosis. Although clinical diagnosis of PD is less ambiguous, biomarkers will allow a deeper understanding of the underlying disease mechanisms to enable early detection, disease monitoring, clinical trial design and biological staging[9]. Disease-specific, quantitative, easily accessible and

e-mail: k.bolsewig@amsterdamumc.nl

cost-efficient fluid biomarkers could support the differential diagnosis of DLB, facilitate DLB and PD research and aid in disease staging and monitoring.

The α-syn seed-amplification assay (αS-SAA) has been shown valuable to detect α-syn pathology already at early disease stages and to predict conversion from nonsymptomatic stages to clinical LBDs[10,11]. αS-SAA-defined co-pathology is present in ~30% of individuals with AD, significantly affecting disease progression and possibly affecting the efficacy of disease-modifying therapies[12,13]. Imaging techniques, such as dopamine transporter (DaT)-Scan, are used to detect nigrostriatal dopaminergic dysfunction[7,14,15], but these costly techniques are often not reimbursed and require the use of radioactive tracers. A fluid biomarker could thus present advantages in terms of costs and safety.

In recent array-based proteomics studies[16–19], the protein DDC was identified as a biomarker candidate for DLB and PD[18]. DDC catalyzes the decarboxylation of L-DOPA to dopamine[20] and 5-HTP to serotonin[21], both of which are impaired in LBDs. DDC levels in CSF were elevated in several LBDs compared with controls and AD, already in early disease stages[17], predicted progression to disease[16–19] and correlated with markers of disease severity[16,17,19]. Blood DDC levels are strongly influenced by dopaminergic treatment and, therefore, do not reflect the presence of LBDs in the central nervous system[22,23]. However, this feature makes it worthy to investigate DDC as a potential biomarker of dopaminergic treatment response. Altogether, these findings strongly suggest DDC as a fluid biomarker to support diagnosis, prognosis and treatment monitoring in LBDs. To translate these findings for use in clinical practice, scalable and accurate laboratory tests measuring absolute DDC concentrations are imperative. While we found that commercial enzyme-linked immunosorbent assay (ELISAs) lack the sensitivity to detect DDC in CSF, a recent preprint reports a mesoscale discovery assay[24], but shows rather high analytical variability (<30%)[24].

Here, we report on the development of two robust immunoassays on highly sensitive immunoassay platforms, Ella and Simoa, for DDC quantification in CSF, plasma and serum. We evaluated the diagnostic potential of CSF DDC for the differentiation of DLB and PD from AD and controls, and analyze associations with αS-SAA status, cognitive dysfunction, DaT imaging, disease severity measures and paired plasma DDC levels. Moreover, we studied DDC tissue expression in relation to relevant pathological features in DLB and PD. Our findings suggest that DDC measured with our immunoassays may serve as a supportive biomarker for the diagnosis of LBDs and gives insights into its association with cognition, clinical features and pathology markers.

Results

DDC biomarker assay development and analytical validation

We developed immunoassays for the detection of DDC in CSF on two platforms: the Ella and Simoa systems (Supplementary Methods 1). The Simoa assay was additionally optimized for use in plasma and serum. All assays demonstrated strong analytical performance, meeting international consensus guidelines[25]. Analytical validation results of the Ella assay (Supplementary Methods 2 and Fig. 1a–e) were an intra-assay coefficient of variation of 4.1%, inter-assay coefficient of variation of 11.5%, parallelism ranging from 85% to 108% (Fig. 1a), dilution linearity between 86% and 117% (Fig. 1b) and spike recovery of 121% (high spike), 85% (medium spike) and 333% (low spike; Fig. 1c). Analytical validation results of the Simoa assay in CSF (Supplementary Methods 2 and Fig. 1f–j) were an intra-assay coefficient of variation of 4.3%, inter-assay coefficient of variation of 12.4%, parallelism ranging from 84% to 87% (Fig. 1f), dilution linearity between 86% and 114% (Fig. 1g) and spike recovery of 95% (high spike), 99% (medium spike) and 84% (low spike; Fig. 1h) and results for the Simoa assay in plasma (Fig. 1k–o) were an intra-assay coefficient of variation of 7.4%, inter-assay coefficient of variation of 12.3%, parallelism ranging from 99% to 101% (Fig. 1k), dilution linearity between 88% and 118% (Fig. 1l) and spike recovery of 95% (high spike), 97% (medium spike) and 70% (low spike; Fig. 1m). In addition, the Simoa assay for use in serum also met the acceptance criteria, results of which are summarized in Extended Data Fig. 1a–e and Supplementary Methods 3.

We measured CSF DDC in six independent cohorts, and in paired plasma samples in one cohort. DDC levels were above the detection limit in 100% of the samples. Demographic characteristics of the included fluid cohorts are summarized in Extended Data Tables 1–3.

In two of these cohorts (Amsterdam Dementia Cohort (ADC) Discovery and UNIPG αS-SAA), we measured CSF DDC with both of the immunoassays. DDC measurements correlated strongly between the two platforms (ADC Discovery: $\rho = 0.95$, $P = 6.06 \times 10^{-73}$; UNIPG αS-SAA: $\rho = 0.842$, $P = 1.13 \times 10^{-58}$), with a proportional difference between the Ella and Simoa measurements, that is, higher absolute concentrations being measured on the Ella assay (Extended Data Fig. 1f,g).

We observed strong correlations between proximity extension assay (PEA) DDC measurements and our in-house-developed assays ($\rho = 0.7–0.97$, $P = 4.86 \times 10^{-37}–1.43 \times 10^{-63}$; Extended Data Fig. 1h–k). Taken together, we have developed two DDC immunoassays for use in CSF (Ella and Simoa) and plasma/serum (Simoa), which demonstrate strong analytical performance and correlate with each other, and PEA results.

DDC concentrations differentiate clinically defined DLB and PD from controls and AD

To assess the diagnostic accuracy of CSF DDC in a memory clinic setting, we first assessed CSF DDC concentrations in clinically defined cohorts from different memory clinics: the ADC Discovery reflects part of the discovery cohort from our previous proteomics study. The ADC/Sant Pau Initiative on Neurodegeneration (SPIN) Validation is a multicenter cohort and was also part of the previous proteomics study (controls, $n = 108$; DLB, $n = 106$; mild cognitive impairment with underlying amyloid pathology (MCI-A+), $n = 101$; AD, $n = 104$). Due to the pathological and clinical similarities between DLB and PD, and previously reported elevated CSF DDC concentrations in both of these diseases, we additionally included a DLB/PD cohort from the Danish Dementia Biobank and Bispebjerg Movement Disorder Biobank (DDBB/BMDB Validation), including patients with DLB and PD. DDC CSF concentrations were significantly elevated in all cohorts within the DLB and PD groups compared to controls (fold changes 1.6 to 2.4) and AD (fold changes 1.2 to 1.9; ADC Discovery Ella: $F(2) = 42.3$, $P = 4.94 \times 10^{-15}$; Simoa: $F(2) = 35.2$, $P = 4.47 \times 10^{-13}$; ADC/SPIN Validation on Ella: $F(3) = 12.0$, $P = 1.51 \times 10^{-7}$; DDBB/BMDB Validation: $F(3) = 33.91$, $P = 2.85 \times 10^{-17}$; Extended Data Table 4 and Fig. 2a–d). We also observed slightly elevated CSF DDC levels in AD compared to controls in ADC/SPIN and DDBB/BMDB Validation. CSF DDC concentrations in PD were slightly elevated compared to DLB in the DDBB/BMDB Validation. Of note, $n = 20$ of these patients with PD (54%) received dopaminergic treatment.

We assessed the potential of CSF DDC for differential diagnosis of DLB and PD from other groups by receiver operating characteristic (ROC) analysis. The models including DDC, age and sex discriminated DLB and PD with area under the curve (AUC) values of 0.94 to 0.97 from controls and with AUCs of 0.70 to 0.94 from patients with AD, independently of the platform used (Fig. 2i–l and Table 1). See model performances for models including DDC, or age and sex, alone in Extended Data Table 5. These results highlight the diagnostic potential of CSF DDC in a clinically defined patient population that reflects individuals commonly seen in memory clinics.

DDC concentrations differentiate biologically and pathologically defined patients with DLB and PD from controls and AD

We next measured CSF DDC in two cohorts including patients with PD + DLB who were biologically confirmed through αS-SAA measurements and patients with DLB who were pathologically confirmed. Also in these cohorts, we observed that CSF DDC was significantly elevated

https://doi.org/10.1038/s41591-026-04212-0

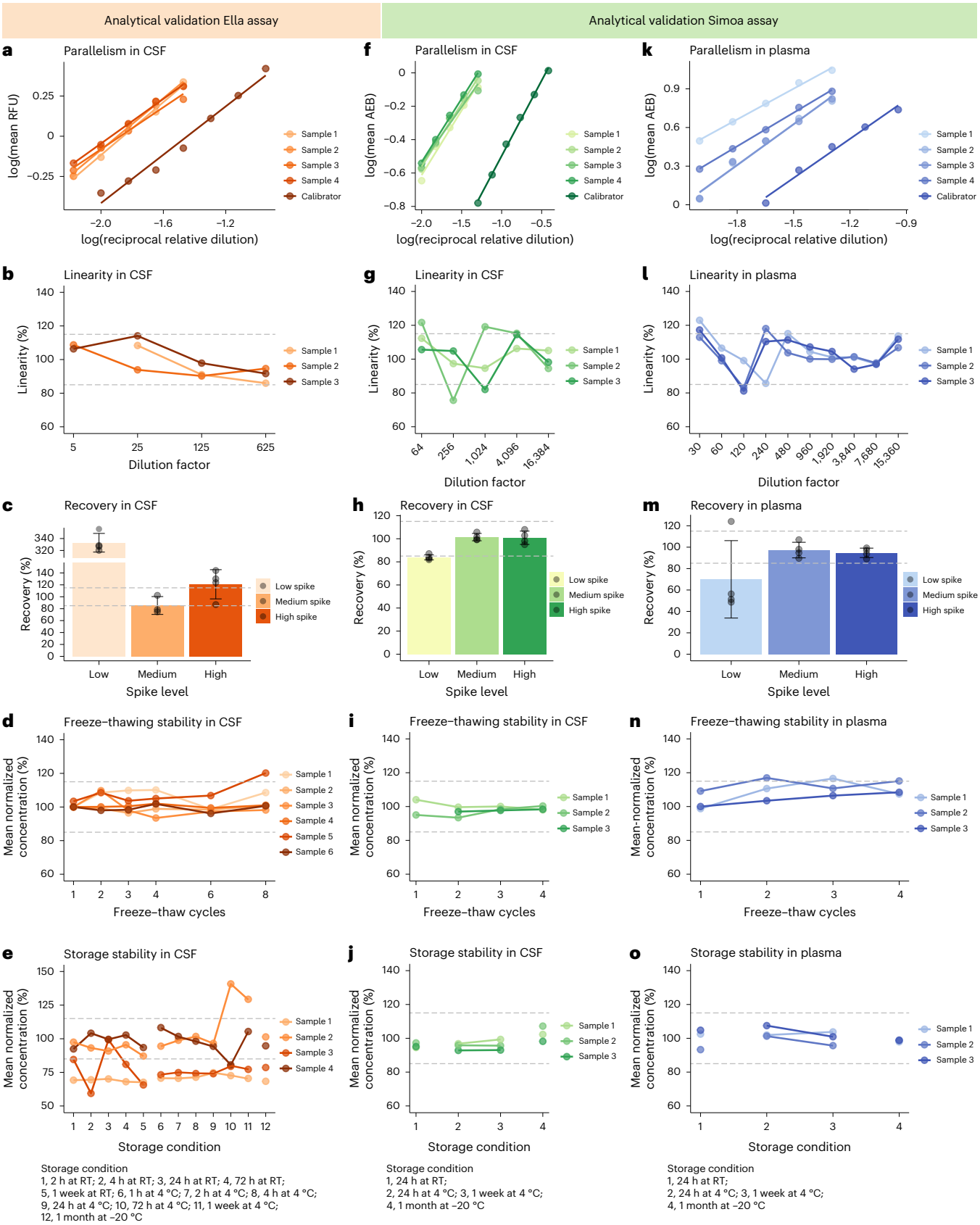

Fig. 1 | Results of analytical validation of Ella and Simoa DDC assays in CSF and plasma. a–**o**, Visual presentation of analytical validation results of the in-house-developed Ella and Simoa assays for the parameters parallelism (**a** (Ella, CSF), **f** (Simoa, CSF) and **k** (Simoa, plasma)), dilution linearity (**b** (Ella, CSF), **g** (Simoa, CSF) and **l** (Simoa, plasma)), recovery (**c** (Ella, CSF), **h** (Simoa, CSF) and **m** (Simoa, plasma)), freeze–thawing stability (**d** (Ella, CSF), **i** (Simoa, CSF) and **n** (Simoa, plasma)) and storage stability (**e** (Ella, CSF), **j** (Simoa, CSF) and **o** (Simoa, plasma)). Mean recovery and corresponding standard deviation (error bars in **c** (Ella, CSF), **h** (Simoa, CSF) and **m** (Simoa, plasma)) were calculated based on three (only medium spike recovery of Ella assay) or four individual CSF or plasma samples. For all parameters, a range of 85% to 115% compared to the reference condition was accepted. AEB, average number of enzymes per bead; RFU, relative fluorescence unit; RT, room temperature.

in the PD + DLB and DLB groups compared with controls (fold changes of 1.8 to 2.2) and AD (fold changes of 1.5 to 1.9; UNIPG αS-SAA on Ella: $F(2) = 38.8$, $P = 4.51 \times 10^{-15}$, and Simoa: $F(2) = 79.7$, $P = 2.92 \times 10^{-27}$; BIODEM/UAntwerp Autopsy: $F(2) = 11.5$, $P = 4.52 \times 10^{-5}$; Fig. 2e–g). Of note, the PD + DLB group in UNIPG αS-SAA included patients on dopaminergic treatment (Extended Data Table 2). Previous studies have shown that dopaminergic treatment can further elevate CSF DDC concentrations. Hence, we repeated the analysis in the UNIPG αS-SAA Cohort stratifying the PD + DLB group for use of dopaminergic treatment. We did not observe differences in CSF DDC levels between the different PD + DLB subgroups (Extended Data Fig. 1l,m), but CSF DDC levels were higher in treated patients compared with drug-naive patients (fold changes 1.2 (Ella) and 1.4 (Simoa)). However, CSF DDC concentrations were still significantly higher in the drug-naive PD + DLB group compared with controls and AD (Fig. 2e,f).

Regarding diagnostic performance, DDC combined with age and sex discriminated PD + DLB with AUCs of 0.89 (Ella) and 0.93 (Simoa) from controls and from patients with AD with AUCs of 0.90 (Ella) and 0.92 (Simoa). ROC analysis in drug-naive patients only, led to slightly lower, yet high AUCs of 0.87 (Ella) and 0.91 (Simoa) for the discrimination from controls and 0.87 (Ella) and 0.90 (Simoa) for the discrimination from AD (Fig. 2m,n and Table 1). In the BIODEM/UAntwerp Autopsy, the AUC was 0.998 for the combined model to discriminate DLB from controls and 0.87 to discriminate DLB from AD (Fig. 2o and Table 1). AUCs for models including only DDC, or age and sex, are reported in Extended Data Table 5. Taken together, the results verify the high diagnostic potential for CSF DDC in biologically and pathologically defined patient groups.

Plasma DDC does not have diagnostic potential

Blood-based biomarkers are less invasive than CSF biomarkers and show high diagnostic potential in AD. Therefore, we next assessed the diagnostic value of plasma DDC in the αS-SAA-defined cohort (UNIPG). We did not observe altered plasma DDC levels between diagnostic groups ($F(2) = 2.8$, $P = 0.066$; without correction for use of dopaminergic treatment), but we observed elevated levels in patients with PD + DLB on dopaminergic treatment (Fig. 2h and Extended Data Table 4). These results underline that plasma DDC is strongly influenced by dopaminergic treatment and holds no diagnostic potential for DLB and PD.

Robustness of results and estimation of reference values

Subsequently, we conducted a meta-analysis combining data from all cohorts, showing large overall effect sizes for the comparison of DLB and PD versus controls (standardized mean difference (SMD) = 1.41 (95% confidence interval (CI) 0.92 to 1.89); $I^2 = 78.7\%$, $P = 0.003$; Fig. 2p), as well as DLB and PD versus AD (SMD = 1.00 (95% CI 0.55 to 1.44); $I^2 = 83.5\%$, $P = 2.36 \times 10^{-6}$; Fig. 2q). These findings indicate that CSF DDC levels are robustly elevated in DLB and PD, with values approximately 1.41 standard deviations higher than in controls and 1.00 standard deviation higher than in AD.

We further evaluated stability of Youden cutoff values. Cutoff values on the Ella platform showed variation, but cutoff values on the Simoa platform were remarkably consistent for the differentiation of DLB and PD from controls (ADC Discovery: 27.1 pg ml^{-1}, DDBB/BMDB Validation$_{DLB}$: 31.1 pg ml^{-1}, DDBB/BMDB Validation$_{PD}$: 31.5 pg ml^{-1}, UNIPG αS-SAA: 29.4 pg ml^{-1}) and from AD (ADC Discovery: 27.7 pg ml^{-1}, DDBB/BMDB Validation$_{DLB}$: 30.1 pg ml^{-1}, DDBB/BMDB Validation$_{PD}$: 30.3 pg ml^{-1}, UNIPG αS-SAA: 28.0 pg ml^{-1}; Extended Data Table 5).

Association with cognition and clinical features

Associations of DDC with cognition were analyzed within the DLB and PD groups. In the ADC Discovery, higher CSF DDC levels were associated with higher Mini-Mental State Examination (MMSE) scores when measured with Simoa (β_{Ella}(s.e.) = −0.35 (0.21), $P = 0.104$, Fig. 3a; β_{Simoa}(s.e.) = −0.51 (0.25), $P = 0.047$, Fig. 3b; of note, estimated values are negative due to transformation of MMSE scores). In a subset of patients with DLB from the ADC Validation ($n = 29$), we observed an association at a trend level of higher CSF DDC levels with lower Montreal Cognitive Assessment (MoCA) scores (β(s.e.) = −9.4 (5.50), $P = 0.100$; Fig. 3d). No associations of CSF DDC with cognitive scores were observed in the other cohorts (Fig. 3c,e–g).

Information on the presence of DLB core features was available in the DLB group of the ADC and SPIN cohorts (Extended Data Table 6). We observed higher CSF DDC levels in patients with DLB presenting with parkinsonian symptoms compared with those without ($\beta = 0.13$ (95% CI: 0.018 to 0.233), $P = 0.023$; Fig. 3h) and in patients with visual hallucinations compared to patients without hallucinations ($\beta = 0.107$ (95% CI: 0.034 to 0.180), $P = 0.005$; Fig. 3i)). No significant associations with DDC have been observed for the presence or absence of the other two DLB core features, that is, fluctuations of cognition and RBD (Fig. 3j,k).

We next assessed if there was a linear association to motor impairment severity, as measured with the unified Parkinson disease rating scale part 3 (UPDRS-III) scale, in UNIPG αS-SAA and YUHS DaT-positron emission tomography (PET). There was no association between DDC concentrations and motor impairment in either cohort (UNIPG: β_{Ella}(s.e.) = −10.30 (10.84), $P = 0.348$; β_{Simoa}(s.e.) = −8.75 (7.35), $P = 0.238$; and YUHS: β(s.e.) = 8.82 (5.06), $P = 0.084$; Fig. 3l–n).

Association with dopaminergic treatment and imaging

As we have observed significantly higher DDC concentrations in patients with PD + DLB under dopaminergic treatment compared to drug-naive patients, we analyzed a possible relation between CSF DDC and dopaminergic treatment dosage expressed as levodopa equivalent daily dosage (LEDD). Information on LEDD was available in the UNIPG αS-SAA and the YUHS DaT-PET cohorts. We did not observe an association between LEDD and CSF DDC concentrations in treated patients of either cohort (UNIPG: β_{Ella}(s.e.) = −0.048 (0.120), $P = 0.696$; β_{Simoa}(s.e.) = −0.152 (0.147), $P = 0.312$; YUHS: β(s.e.) = −0.094 (0.210), $P = 0.657$).

Fig. 2 | CSF DDC levels across diagnostic groups and ROC analysis. a–h, Box plots illustrate DDC levels across diagnostic groups in the ADC Discovery (CTRL, $n = 50$; DLB, $n = 41$; AD, $n = 51$; **a** (CSF Ella) and **b** (CSF Simoa)), ADC/SPIN Validation (CTRL, $n = 108$; DLB, $n = 106$; MCI-A+, $n = 101$; AD, $n = 104$; **c**), DDBB/BMDB Validation (CTRL, $n = 44$; DLB, $n = 46$; PD, $n = 37$; AD, $n = 52$; **d**), UNIPG αS-SAA (CSF Ella: CTRL, $n = 51$; PD + DLB (DN), $n = 36$; PD + DLB (T), $n = 19$; AD, $n = 110$ (**e**); CSF Simoa: CTRL, $n = 60$; PD + DLB (DN), $n = 48$; PD + DLB (T), $n = 27$; AD(S−), $n = 110$ (**f**)), BIODEM/UAntwerp Autopsy (CTRL, $n = 30$; DLB, $n = 18$; AD, $n = 30$; **g**) and the plasma UNIPG αS-SAA (CTRL, $n = 18$, PD + DLB (DN), $n = 32$; PD + DLB (T), $n = 20$; AD, $n = 22$; **h**). **i–o**, ROC curves for the differentiation of DLB and PD from the other diagnostic groups based on DDC levels are shown for the ADC Discovery (**i** (CSF Ella) and **j** (CSF Simoa)), ADC/SPIN Validation (**k**), DDBB/BMDB Validation (**l**), UNIPG αS-SAA in CSF (**m** (CSF Ella) and **n** (CSF Simoa)) and the BIODEM/UAntwerp Autopsy (**o**). **p**,**q**, Meta-analyses of SMDs between DLB and PD and controls (**p**) and AD-continuum (**q**) are visualized by forest plots. DDC differences between diagnostic groups were assessed across groups by analysis of covariance (ANCOVA) corrected for age and sex (and center in ADC/SPIN Validation) with two-sided post hoc Tukey's test and Bonferroni correction. Box plots show DDC levels across diagnostic groups. Lines through the boxes indicate the median value, and lower and upper lines correspond to the first and third quartiles, respectively. Dots represent individual data points, and whiskers extend to 1.5 times the interquartile range. Forest plots indicate the SMD of two-sided group comparisons in different diagnostic cohorts and whiskers indicate confidence intervals. Diamonds indicate the pooled effects with confidence intervals. DN, drug-naive; MCI-A+, mild cognitive impairment with underlying amyloid pathology; S−, normal seed-amplification assay; S+, abnormal seed-amplification assay; T, treated with dopaminergic medication.

https://doi.org/10.1038/s41591-026-04212-0

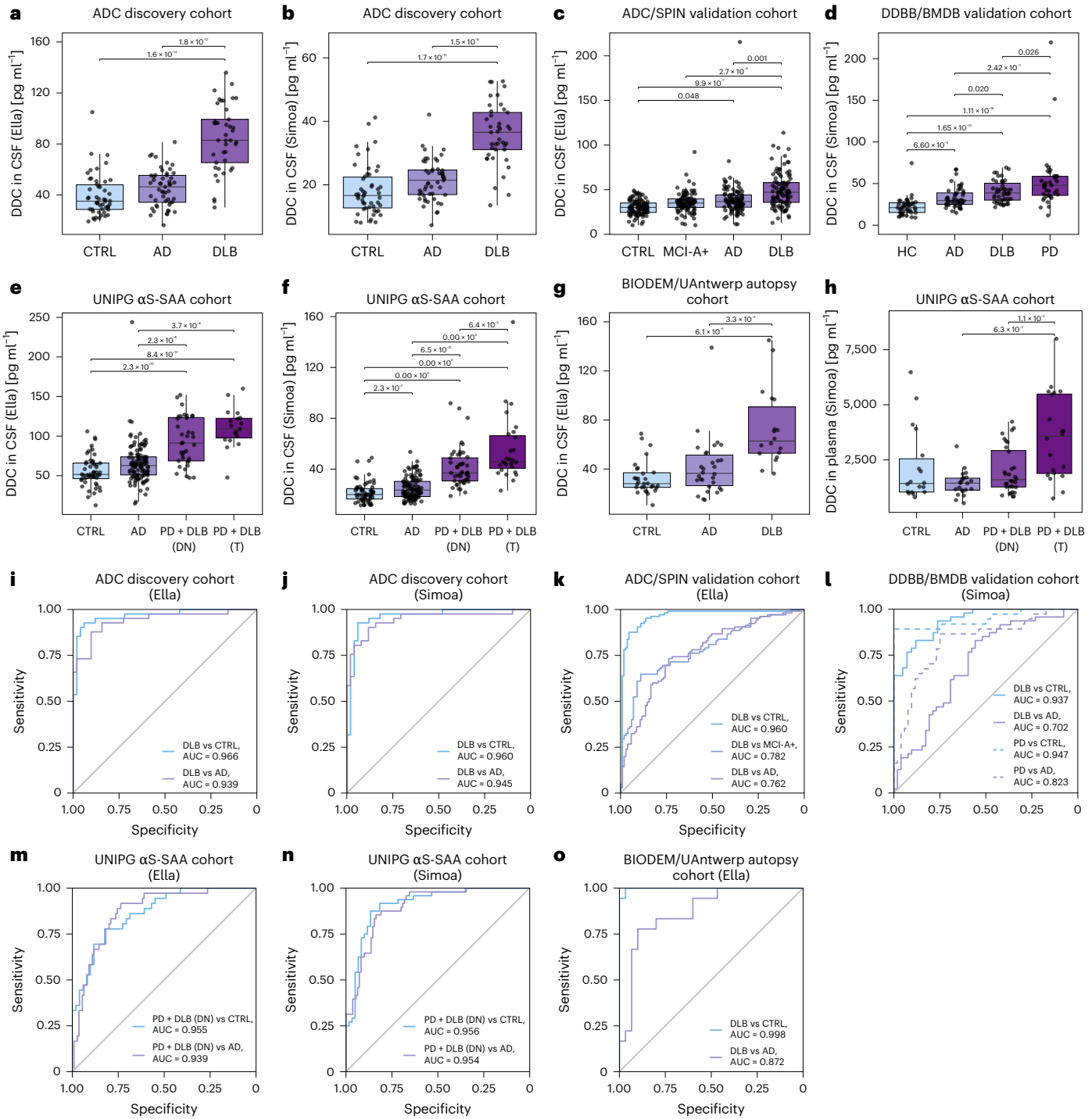

https://doi.org/10.1038/s41591-026-04212-0

Table 1 | Accuracy parameters of ROC analysis. Predictors include age, sex and log_{10}-transformed DDC concentrations

Cohort		AUC	Specificity	Sensitivity	Positive predictive value	Negative predictive value
ADC Discovery Cohort (CSF, Ella)	DLB versus CTRL	0.966	0.94	0.93	0.93	0.94
	DLB versus AD	0.939	0.90	0.88	0.88	0.90
ADC Discovery Cohort (CSF, Simoa)	DLB versus CTRL	0.960	0.94	0.93	0.93	0.94
	DLB versus AD	0.945	0.88	0.90	0.86	0.92
ADC/SPIN Validation Cohort (CSF, Ella)	DLB versus CTRL	0.960	0.95	0.88	0.95	0.89
	DLB versus MCI-A+	0.782	0.89	0.64	0.86	0.71
	DLB versus AD	0.762	0.73	0.72	0.74	0.73
DDBB/BMDB Validation Cohort (CSF, Simoa)	DLB versus CTRL	0.937	0.88	0.83	0.89	0.82
	DLB versus AD	0.702	0.56	0.83	0.63	0.78
	PD versus CTRL	0.947	1	0.89	1.00	0.91
	PD versus AD	0.823	0.75	0.86	0.71	0.89
UNIPG αS-SAA Cohort (CSF, Ella)	PD+DLB versus CTRL	0.894	0.88	0.89	0.88	0.78
	PD+DLB versus AD	0.895	0.78	0.91	0.68	0.95
	PD+DLB (DN) versus CTRL	0.867	0.82	0.78	0.76	0.84
	PD+DLB (DN) versus AD	0.872	0.74	0.92	0.53	0.96
UNIPG αS-SAA Cohort (CSF, Simoa)	PD+DLB versus CTRL	0.930	0.88	0.93	0.79	0.91
	PD+DLB versus AD	0.917	0.84	0.88	0.79	0.91
	PD+DLB (DN) versus CTRL	0.910	0.87	0.88	0.84	0.90
	PD+DLB (DN) versus AD	0.897	0.84	0.85	0.69	0.93
BIODEM/UAntwerp Autopsy Cohort (CSF, Ella)	DLB versus CTRL	0.998	0.97	1.00	0.95	1.00
	DLB versus AD	0.872	0.90	0.78	0.82	0.87

CTRL, controls; DN, drug-naive.

We further assessed if CSF DDC measurements are related to DaT imaging. DaT-Scan results were available for a subset of the DLB group in the ADC and SPIN cohorts (Extended Data Table 6). There was no significant difference in DDC concentrations within the DLB group between patients with normal ($n = 10$) or abnormal ($n = 38$; $F(1) = 0.170$, $P = 0.683$, $\beta = 0.026$ (95% CI: −0.102 to 0.154); Fig. 3o) DaT-Scan results. Similar results were found in the YUHS DaT-PET regarding DaT-PET status (normal = 24, abnormal = 78, $F(1) = 0.279$, $P = 0.598$, Fig. 3p and Supplementary Methods 4). We did not observe an association between CSF DDC levels and DaT uptake, as represented by median ^{18}F-FP-CIT PET standardized uptake value ratios, in the caudate or putamen within the whole cohort ($n = 102$) or only drug-naive patients ($n = 60$), respectively (Extended Data Table 7 and Fig. 3q,r). However, we observed that higher CSF DDC levels were associated with a lower caudate/putamen DaT uptake ratio in drug-naive patients (β(s.e.) = −0.201 (0.060), $P = 0.0015$, $q = 0.0045$; Extended Data Table 7 and Fig. 3s).

Association with AD co-pathology

Since CSF DDC concentrations were also elevated in patients with AD and AD co-pathology is a common feature in DLB and PD, we assessed the relationship between CSF DDC and AD pathology based on the AD CSF core biomarkers $A\beta_{42}$ (ADC, DDBB/BMDB Validation and BIODEM/UAntwerp Autopsy) or $A\beta_{42/40}$ (SPIN, UNIPG αS-SAA), pTau181 (all cohorts) and tTau (all cohorts) in the overall cohorts and the DLB and PD groups, respectively.

DDC was negatively associated with amyloid in the ADC/SPIN Validation. In patients from the ADC, CSF DDC was associated with $A\beta_{42}$ within all diagnoses together (β(s.e.) = −0.11 (0.05), $P = 0.028$), and in patients with DLB from the SPIN, DDC was associated with $A\beta_{42/40}$ (β(s.e.) = −2.09 (0.87), $P = 0.020$). DDC and pTau were positively associated in the PD + DLB group of the UNIPG αS-SAA (Simoa, β(s.e.) = 0.26 (0.12), $P = 0.026$). In the BIODEM/UAntwerp Autopsy, a positive association of DDC and tTau was observed in the whole cohort (β(s.e.) = 0.21 (0.10), $P = 0.037$), while in the DDBB/BMDB Validation a positive association was observed in the PD group (β(s.e.) = 0.54 (0.16), $P = 0.007$). When stratifying for AD CSF biomarker status, we confirmed that amyloid-positive patients with DLB had higher CSF DDC levels than amyloid-negative patients in ADC/SPIN Validation ($F(1) = 7.7$, $P = 0.007$; $\beta = 0.09$ (95% CI: 0.02–0.15)). Besides that, AD CSF biomarker-positive patients had similar CSF DDC levels compared with AD CSF biomarker-negative patients. Overall, while associations between CSF DDC and certain AD CSF biomarkers were observed in some cohorts, these findings were not consistent across all study cohorts.

Association with α-syn pathology

To assess the association of CSF DDC with α-syn, we first analyzed if elevated CSF DDC levels in AD are related to LB pathology by comparing DDC concentrations between αS-SAA normal ($n = 54$) and αS-SAA abnormal ($n = 56$) patients with AD. CSF DDC levels did not significantly differ regarding the αS-SAA status, but a trend toward higher CSF DDC in αS-SAA positive patients with AD was observed when measured by Simoa (β_{Ella}(s.e.) = −1.31 (4.97), $P = 0.793$; β_{Simoa}(s.e.) = 2.41 (1.59), $P = 0.134$; Fig. 4a,b). We next evaluated this relation in pathologically confirmed patients with AD within the BIODEM/UAntwerp Autopsy. Here, patients with AD and LB co-pathology had higher CSF DDC concentrations than patients with pure AD (β(s.e.) = 0.21 (0.08), $P = 0.014$; Fig. 4c). Next, we analyzed CSF DDC levels in relation to LB pathology, based on the regional LB stage, α-syn Braak stages and α-syn load in different brain areas. We observed higher CSF DDC levels in patients (DLB and AD) with LB pathology in the limbic and neocortical brain areas compared to patients with AD without LB co-pathology ($F(3) = 5.64$, $P = 0.002$; Fig. 4d) and higher CSF DDC levels were associated with higher α-syn Braak stages ($F(5) = 5.05$, $P = 0.001$; Fig. 4e). In addition, CSF DDC correlated with α-syn load in various brain regions, with the strongest correlation in the substantia nigra ($P = 0.66$, $P = 5.36 \times 10^{-7}$; Fig. 4f).

These results indicate that CSF DDC concentrations increase with disease progression and with increasing LB pathology, particularly in the brainstem.

DDC characterization in human brain tissue

As results from the BIODEM/UAntwerp Autopsy suggest an association of higher CSF DDC concentrations with more pronounced LB pathology in specifically the brainstem (substantia nigra), we next analyzed the (co)localization of DDC and α-syn within brainstem tissue from controls ($n = 4$), patients with DLB ($n = 4$) and PD (dementia) (PD(D); $n = 4$), using the detection antibody of our immunoassays. Demographics and neuropathological characteristics of the tissue donors are listed in Extended Data Table 8. Of note, staining was interpreted qualitatively by visual inspection to assess presence, distribution and relative intensity of the target antigens. Positive DDC signal was detected within the nucleus, soma and processes of dopaminergic neurons, as indicated by overlapping DDC, tyrosine hydroxylase (stains dopaminergic neurons) and neuromelanin (abundant in dopaminergic neurons of substantia nigra) positivity in these cells (Fig. 5a–g and Extended Data Fig. 2a–f). Positive DDC staining was sparsely observed in tyrosine hydroxylase-negative cells in all groups. Positive DDC signal was also detected in the nucleus, soma and processes of serotonergic neurons in the raphe nuclei (Supplementary Methods 5 and Extended Data Fig. 2g–j). In all patients, DDC positivity was present within LBs, LNs and pale bodies in dopaminergic neurons (Fig. 5e–g,l,m,p,q,t,u). Furthermore, DDC colocalized with phosphorylated Ser129 α-syn staining in these neurons (Fig. 5h–w). While fewer DDC-positive cells were observed in the DLB and PD groups, strong DDC signal was observed in the nucleus and soma of remaining neurons and within LBs and LNs. These findings show that DDC colocalizes with α-syn, that tyrosine hydroxylase-negative cells still express DDC and that DDC is also detected in serotonergic neurons.

Discussion

In the present study we show the clinical value of CSF DDC as a biomarker for DLB and PD and introduce two quantitative immunoassays advancing clinical implementation. We developed two robust in-house immunoassays to measure DDC in CSF (and plasma and serum) with high analytical sensitivity (100% detectability) and excellent technical performance, correlating strongly with PEA measurements. We validated the use of CSF DDC in six cohorts: three clinical cohorts, one DaT imaging cohort, one biologically defined cohort and one autopsy-confirmed DLB and PD patient cohort, consistently showing significantly elevated CSF DDC levels in the DLB and PD groups and demonstrating high AUCs of up to 0.93 for differential diagnosis throughout. Stable cutoff values of ~30 pg ml^{-1}, to differentiate DLB and PD from the other groups, were observed with the Simoa assay. Within participants that largely presented with cognitive impairment and parkinsonian symptoms, CSF DDC was not associated with normal/abnormal DaT imaging status, but higher CSF DDC was associated with a lower caudate/putamen DaT uptake ratio. Higher CSF DDC values were related with the presence of parkinsonism and visual hallucinations in DLB, but were not associated with motor impairment severity in PD + DLB. Furthermore, we show that CSF DDC concentrations increased with more pronounced α-syn pathology, that DDC colocalized with phosphorylated Ser129 α-syn, and show DDC positivity in dopaminergic and serotonergic neurons in human postmortem brainstem tissue.

We show that CSF DDC was significantly elevated in DLB and PD compared with controls, MCI-A+ and AD, and our meta-analysis showed strong pooled effect sizes for the comparison of DLB and PD versus controls and DLB and PD versus AD, which further underscores the robustness of DDC differences across diagnostic groups. Upon addition of DDC to basic demographic models including age and sex as predictors, these AUCs increased further, reaching 0.97 in clinically defined cohorts and 0.998 in the autopsy-confirmed cohort. These findings are in concordance with previous proteomics studies[16], but now measured by scalable methods, with stable cutoff values advancing clinical implementation. We observed slightly higher CSF DDC concentrations in patients receiving dopaminergic treatment compared to drug-naive patients, both in CSF and plasma. Similar findings have been reported previously[17,19,23]. However, DDC levels in CSF were still significantly upregulated in drug-naive patients, and this factor can likely be disregarded in the context of initial diagnosis, as patients will still be drug-naive. Upregulation was only observed in plasma of dopaminergic-treated patients, confirming our previous findings on limited diagnostic utility in plasma[22]. Our findings suggest that CSF DDC is a promising biomarker to support clinical DLB and PD diagnosis, ultimately facilitating and improving the diagnostic process.

CSF DDC levels were slightly elevated in patients with AD (fold change up to 1.5). LB co-pathology is a frequent feature observed in ~30% of patients with AD[26–28] as confirmed by CSF αS-SAA analysis[12,13]. In the BIODEM/UAntwerp Autopsy, we observed that patients with AD and LB co-pathology had significantly higher CSF DDC levels than those patients with pure AD. When using the αS-SAA, we observed trend-level differences in patients with AD with or without LB pathology. These findings suggest that LB co-pathology in AD might not be the only cause for elevated DDC levels in AD, or may affect CSF DDC differently than in DLB/PD. One possible explanation is that AD and DLB/PD affect distinct brain regions, potentially dysregulating DDC expression in different ways even when LB co-pathology is present. Additionally, since DDC is also involved in serotonin synthesis, and serotonin deficits occur both in DLB/PD and AD, this could contribute to increases in CSF DDC levels in pure AD cases. Elevated CSF DDC levels have also

Fig. 3 | Associations of DDC with cognition, DLB core features, motor impairment and DaT imaging. a–s, DDC levels were borderline associated with MMSE in the ADC Discovery (**a** (Ella) and **b** (Simoa)), but not in the ADC/SPIN Validation (**c**) and the DDBB/BMDB Validation (**e**), or with MoCA in the ADC Validation (**d**) and UNIPG αS-SAA (**f** (Ella) and **g** (Simoa)) within DLB and PD (DLB ADC Discovery, $n = 41$; DLB ADC/SPIN Validation, $n = 106$; DLB DDBB/BMDB Validation, $n = 46$; PD DDBB/BMDB Validation, $n = 37$; PD + DLB UNIPG αS-SAA (CSF Ella), $n = 55$; PD + DLB UNIPG αS-SAA (CSF Simoa), $n = 75$). Associations of CSF DDC with DLB core features were analyzed within the DLB group of the ADC/SPIN Validation. Patients with DLB that presented with parkinsonism (**h**; $n = 70$) or visual hallucinations (**i**; $n = 48$) had higher CSF DDC levels than patients without these features (n without parkinsonism = 11, n without hallucinations = 31). No association was observed between CSF DDC and the other core features fluctuations of cognition (n with fluctuations of cognition = 53, n without fluctuations of cognition = 18; **j**) and RBD (n with RBD = 42, n without RBD = 32; **k**). No association with CSF DDC and UPDRS-III scores was observed in the UNIPG αS-SAA (n Ella = 55, n Simoa = 75; **l** (Ella) and **m** (Simoa)) or YUHS DaT-PET ($n = 102$; **n**). CSF DDC did not differ between DaT imaging normal and abnormal status (n DaT-Scan normal/abnormal = 10/38 (**o**), n DaT-PET normal/abnormal = 24/78 (**p**)). In drug-naive patients ($n = 60$), no association between CSF DDC and ^{18}F-FP-CIT uptake in the caudate (**q**) or putamen (**r**) was observed, respectively, but higher CSF DDC concentrations were associated with lower caudate/putamen ^{18}F-FP-CIT uptake ratios (**s**). Associations with cognitive scores and median ^{18}F-FP-CIT standardized uptake value ratio (SUVRs) were assessed by linear regression corrected for age, sex and education (when available) and associations with UPDRS-III scores were assessed by linear regression corrected for age, sex, LEDD and disease duration. Regression lines with 95% CIs of cognition models are presented in DLB (light red), PD (dark red) and PD + DLB (red) and of models for motor impairment in PD + DLB (gray). Associations of CSF DDC with clinical DLB core features and DaT imaging status were assessed by ANCOVA, corrected for age and sex, with two-sided post hoc Tukey's test. Box plots represent DDC levels, lines through the boxes represent the median value, and lower and upper lines correspond to the first and third quartiles, respectively. Dots represent individual data points and whiskers extend to 1.5 times the interquartile range. Adj., adjusted.

https://doi.org/10.1038/s41591-026-04212-0

been shown in atypical parkinsonian disorders (multiple system atrophy, progressive supranuclear palsy, corticobasal syndrome), albeit lower than in LBD[17]. These disorders, similarly to DLB and PD, exhibit varying degrees of dopamine and serotonin deficits. However, they do not have underlying α-syn pathology (progressive supranuclear palsy and corticobasal syndrome[29]), or in the case of multiple system atrophy, α-syn pathology differs from that observed in DLB and PD to an extent that it can be challenging to detect it with αS-SAA[30–32]. Therefore,

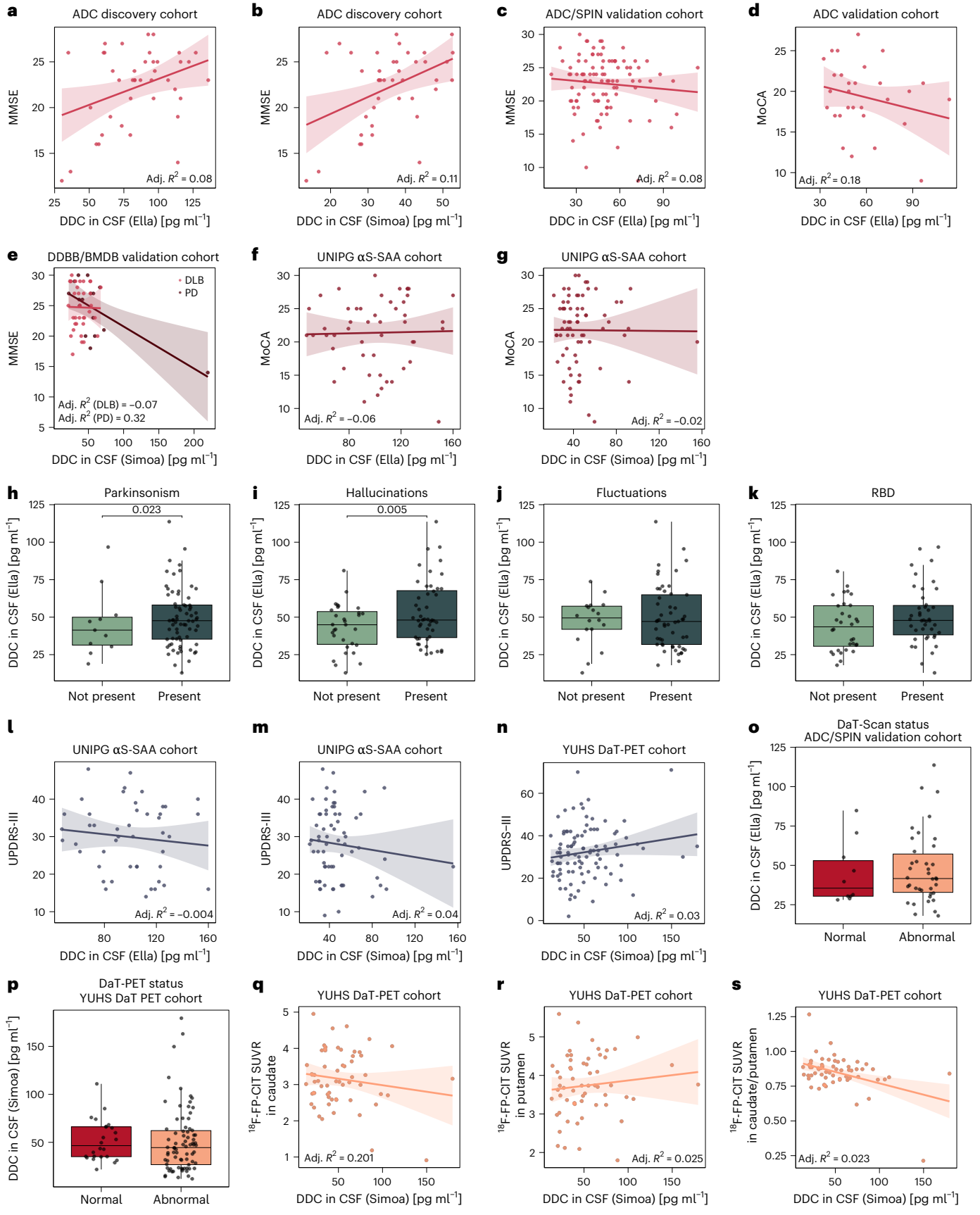

https://doi.org/10.1038/s41591-026-04212-0

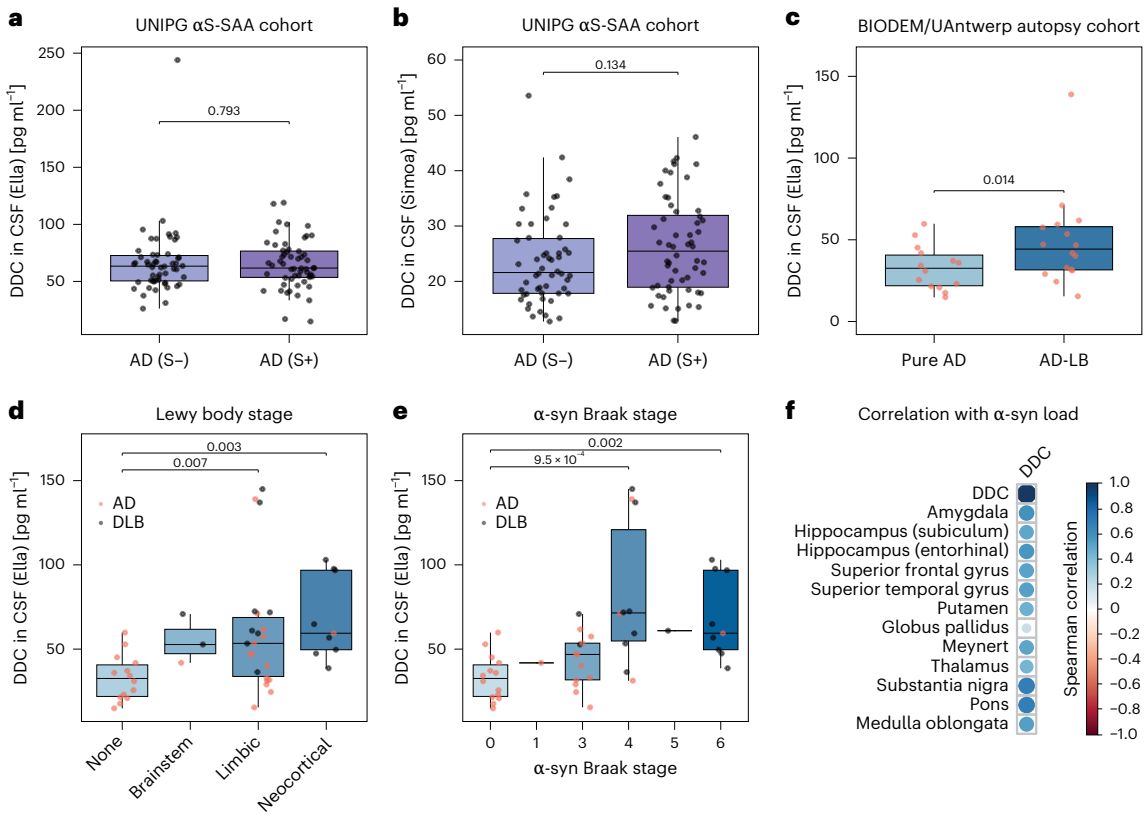

Fig. 4 | Associations of CSF DDC with α-syn pathology. a–f, In the UNIPG αS-SAA Cohort, no significant difference of CSF DDC was observed between αS-SAA normal ($n = 54$) and αS-SAA abnormal ($n = 56$; **a** (Ella) and **b** (Simoa)) patients with AD. In the BIODEM/UAntwerp Autopsy Cohort (DLB, $n = 18$; AD, $n = 30$), higher CSF DDC levels were associated with LB co-pathology in AD (**c**), Lewy pathology in the limbic and neocortical brain areas (**d**) and higher α-syn Braak stages (**e**), and correlated with α-syn load in various brain regions (**f**). Associations of CSF DDC with αS-SAA status, LB co-pathology in AD, Lewy pathology and α-syn Braak stages were assessed by ANCOVA, corrected for age and sex, with two-sided post hoc Tukey's test. Box plots represent DDC levels, lines through the boxes represent the median value, and lower and upper lines correspond to the first and third quartiles, respectively. Dots represent individual data points, and whiskers extend to 1.5 times the interquartile range. Correlation of CSF DDC with α-syn load was analyzed in different brain regions by Spearman correlation. Positive correlation coefficients are indicated by the blue color and the size of the dots indicates strength of correlation. S−/S+, αS-SAA normal/abnormal.

CSF DDC could possibly be a valuable biomarker to better define and distinguish these atypical parkinsonian syndromes from each other, which requires more research. Following this hypothesis, it may also be worth investigating CSF DDC in psychiatric disorders affecting the dopaminergic and serotonergic systems, such as major depressive disorder[33] or schizophrenia, particularly considering the fact that DDC is also involved in the production of serotonin[20].

Dopaminergic imaging by DaT-Scan is a supportive biomarker for the diagnosis of DLB. We did not observe an association between CSF DDC and normal/abnormal DaT-Scan and DaT-PET, nor with DaT uptake in the caudate or putamen in patients with DLB, respectively, in line with previously reported findings for DDC in PD[24,34]. However, we observed that higher CSF DDC concentrations were associated with lower caudate/putamen DaT uptake ratios. Previous studies have shown that patients with DLB present with lower caudate/putamen DaT uptake ratios than patients with PD[35,36]. Given that almost all participants in the YUHS DaT-PET cohort were cognitively impaired with additional parkinsonian symptoms, we hypothesize that here elevated CSF DDC may reflect more widespread dopaminergic degeneration, including involvement of the caudate nucleus, likely related to the presence of cognitive impairment and, consistent with a DLB-like dopaminergic pattern, in contrast to a pattern involving mainly the putamen in PD.

In pathologically confirmed patients, we observed higher CSF DDC levels in patients with limbic and neocortical LB stages compared to patients with AD without LB pathology. Additionally, CSF DDC was associated with higher α-syn Braak stages and correlated with α-syn load in various brain regions, particularly in the substantia nigra, corroborating our previous findings[16]. Our findings further show that DDC colocalizes with phosphorylated Ser129 α-syn in the substantia nigra. While colocalization alone does not confirm a functional interaction, this spatial proximity, particularly within LBs and LNs, raises the possibility of an interplay between these proteins. α-synuclein pathology has been proposed to possibly interfere with the dopaminergic pathway, by increasing the risk of developing neuronal dopaminergic dysfunction[2]. This rationale is further supported by findings of previous studies that associated abnormal α-syn production with decreased DDC activity[37]. A decrease in DDC activity and resulting shortage of dopamine could lead to a compensatory overproduction of DDC in remaining neurons, which could be an explanation for the elevated concentrations observed in CSF, as suggested previously[19]. Supporting this hypothesis is the here-observed positive correlation of CSF DDC levels with α-syn in the substantia nigra, where loss of dopaminergic neurons is most pronounced. A positive correlation between CSF DDC and α-syn could hence indicate an overproduction of DDC in the remaining neurons. Another possible explanation for elevated CSF DDC could be ongoing degeneration of dopaminergic neurons in DLB and PD, leading to release of DDC into the extracellular matrix and CSF. This explanation is supported by our observation of fewer dopaminergic neurons within DLB and PD(D) substantia nigra brain tissue compared with controls. DDC was also detected in tyrosine hydroxylase-negative cells. Tyrosine hydroxylase negativity can be observed when dopaminergic cell degeneration processes start and the cells initiate cytoprotective

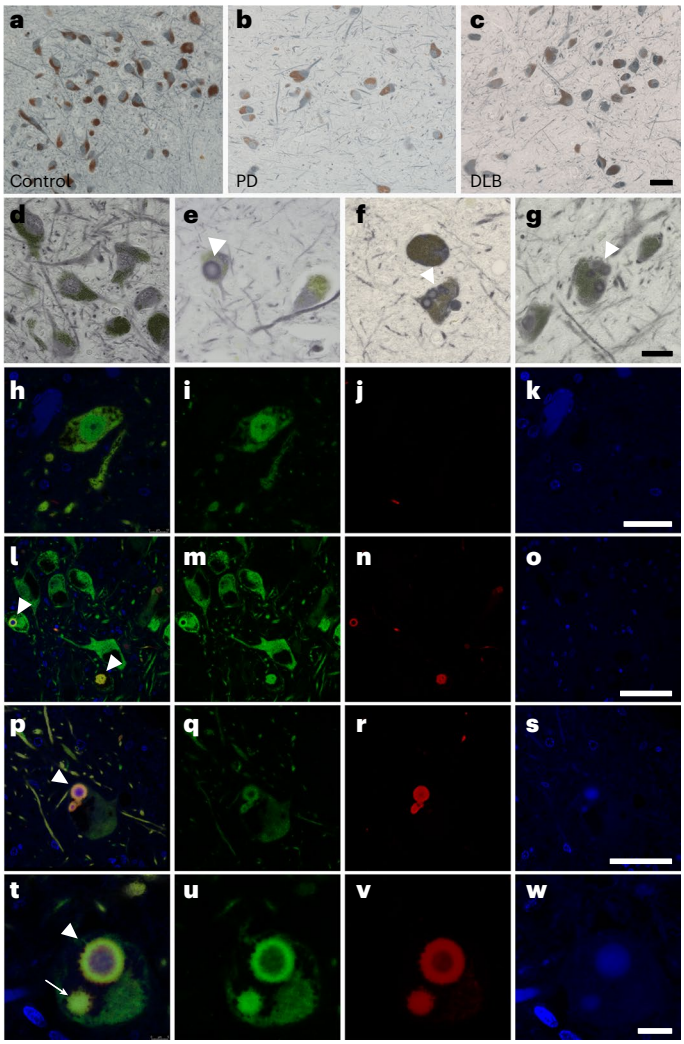

Fig. 5 | DDC immunohistochemical staining (DDC+) in postmortem substantia nigra tissue. a–**w**, DDC (gray) was detected in the nucleus, soma and processes of dopaminergic neurons (neuromelanin in brown) in control (**a** and **d**), PD(D) and DLB donors (**b**, **c**, **h** and **i**). In PD(D) and DLB donors, some neurons showed single or multiple DDC-positive LBs (**e**–**g**; arrowhead). Multi-labeling confirmed colocalization of DDC (green; **i**, **m**, **q** and **u**) with phosphorylated Ser129 α-syn (red; **j**, **n**, **r** and **v**) in pale bodies (arrow), LBs (arrowhead) and LNs in the substantia nigra. Nuclei were stained with DAPI (blue; **k**, **o**, **s** and **w**). Overlay of DDC, phosphorylated Ser129 α-syn and DAPI is shown in **h**, **l**, **p** and **t**. Stainings were performed in postmortem brain tissue from neurologically healthy controls ($n = 4$), patients with DLB ($n = 4$) and patients with PD(D) ($n = 4$; Extended Data Table 8). Representative stainings are shown for $n = 1$ control, $n = 1$ patient with PD and $n = 3$ patients with DLB. **a**–**g**, Brightfield microscopy images of single-DDC labeling. **h**–**w**, Fluorescence microscopy of multi-DDC/phosphorylated Ser129 α-syn/DAPI labeling. **a**,**d**, Control, 20× and 60× magnification, respectively. **b**,**e**, PDD, 20× and 60× magnification, respectively. **c**,**f**,**g**, DLB, 20× and 60× magnification, respectively. **h**,**l**,**p**,**t**, Overlay of multi-DDC/phosphorylated Ser129 α-syn/DAPI labeling in different regions. **i**,**j**,**k**, Isolated DDC (**i**), phosphorylated Ser129 α-syn (**j**) and DAPI (**k**) signal corresponding to the overlaid image in **h**. **m**,**n**,**o**, Isolated DDC (**m**), phosphorylated Ser129 α-syn (**n**) and DAPI (**o**) signal corresponding to the overlaid image in **l**. **q**,**r**,**s**, Isolated DDC (**q**), phosphorylated Ser129 α-syn (**r**) and DAPI (**s**) signal corresponding to the overlaid image in **p**. **u**,**v**,**w**, Isolated DDC (**u**), phosphorylated Ser129 α-syn (**v**) and DAPI (**w**) signal corresponding to the overlaid image in **t**. DAPI, 4′,6-diamidin-2-phenylindol; PD(D), Parkinson's disease (dementia). Scale bars: 50 µm (**a**–**c**,**p**–**s**), 10 µm (**d**–**g**,**t**–**w**), 25 µm (**h**–**k**), 75 µm (**l**–**o**).

processes[38]. In addition to these findings in dopaminergic neurons, we also observed positive staining for DDC in serotonergic neurons of the raphe nuclei. Together, these findings suggest that measured CSF DDC may reflect both dopaminergic and serotonergic dysfunction to some extent. However, the underlying reasons for elevated CSF DDC, as well as the extent to which α-syn pathology and impairment of the nigrostriatal dopaminergic and serotonergic pathway are interconnected and influence CSF DDC levels, remain to be elucidated.

Elevated CSF DDC levels were associated with clinical symptoms, such as the presence of parkinsonism and visual hallucinations in patients with DLB. While the molecular mechanism causing visual hallucinations is not yet understood, the observed associations are in line with our findings of higher CSF DDC in relation to LB pathology in the limbic and neocortical brain regions, which are involved in, for example, sensory processing, emotion and perception[39,40]. While parkinsonian symptoms are known to be directly caused by nigrostriatal dopaminergic dysfunction, the lack of association of DDC levels with continuous UPDRS-III scores tentatively suggests that CSF DDC levels may not be directly related to nigrostriatal dopaminergic degeneration. We did not observe consistent associations of DDC with cognitive impairment or AD CSF biomarkers, corroborating previous findings suggesting rather weak correlations between these clinical symptoms and biological disease severity[16–19]. Future studies should thoroughly assess how DDC associates with clinical disease parameters.

To allow for the implementation of biomarkers into clinical and research practice, quantification of absolute protein concentrations is essential, which is a common limitation of biomarker discovery technologies, including PEA. Nevertheless, using antibody-based discovery approaches, as applied for DDC, increased success rates and shortened the time to develop a biomarker assay ready for clinical implementation, as shown here and before[41–43].

Our study has limitations. We cannot exclude misdiagnosis of DLB cases. However, clinical diagnoses were made by DLB experts according to consensus guidelines[7], and in two cohorts confirmed by αS-SAA or neuropathology, and DDC findings were consistent across cohorts. Further, data availability for certain severity measures was limited. These results should hence be seen as a starting point for more extensive studies. Most patients in the YUHS DaT-PET presented with parkinsonian symptoms and multiple co-pathologies. In addition, the study lacked a control group of cognitively unimpaired individuals. As a result, we were unable to compare CSF DDC levels with DaT uptake in pathological versus healthy conditions. To advance clinical implementation, future studies should evaluate diagnostic performance in longitudinal and prospective cohorts, including different disease stages, as well as analyzing the association of CSF DDC with serotonergic dysfunction in different diseases.

In conclusion, our data show strong evidence for DDC as a biomarker to support the clinical diagnosis of DLB and PD: (1) we showed substantially elevated levels in DLB and PD versus controls or patients with AD, and we verified elevated CSF DDC in DLB and PD patients who were confirmed by ex vivo and postmortem gold standards; (2) we assured robustness of our quantitative immunoassays and consistency of measurements by analytical validation according to consensus guidelines[25]; (3) we confirmed specificity of the detection antibody used in the immunoassays by immunostainings in human brain tissue and showed DDC upregulation in remaining dopaminergic neurons and colocalization with phosphorylated Ser129 with α-syn aggregation. Altogether, we propose CSF DDC as a biomarker to support the diagnosis of DLB and PD. Our robust immunoassays offer accessible tools to accurately quantify DDC, advancing possible future implementation of DDC.

Online content

Any methods, additional references, Nature Portfolio reporting summaries, source data, extended data, supplementary information, acknowledgements, peer review information; details of author contributions and competing interests; and statements of data and code availability are available at https://doi.org/10.1038/s41591-026-04212-0.

References

1. Galasko, D. Lewy body disorders. *Neurol. Clin.* **35**, 325–338 (2017).
2. Simuni, T. et al. A biological definition of neuronal alpha-synuclein disease: towards an integrated staging system for research. *Lancet Neurol.* **23**, 178–190 (2024).
3. Hoglinger, G. U. et al. A biological classification of Parkinson's disease: the SynNeurGe research diagnostic criteria. *Lancet Neurol.* **23**, 191–204 (2024).
4. Okitsu, M. et al. Degeneration of nigrostriatal dopaminergic neurons in the early to intermediate stage of dementia with Lewy bodies and Parkinson's disease. *J. Neurol. Sci.* **449**, 120660 (2023).
5. Schulz-Schaeffer, W. J. The synaptic pathology of alpha-synuclein aggregation in dementia with Lewy bodies, Parkinson's disease and Parkinson's disease dementia. *Acta Neuropathol.* **120**, 131–143 (2010).
6. Postuma, R. B. et al. MDS clinical diagnostic criteria for Parkinson's disease. *Mov. Disord.* **30**, 1591–1601 (2015.
7. McKeith, I. G. et al. Diagnosis and management of dementia with Lewy bodies: fourth consensus report of the DLB Consortium. *Neurology* **89**, 88–100 (2017).
8. Zaccai, J., McCracken, C. & Brayne, C. A systematic review of prevalence and incidence studies of dementia with Lewy bodies. *Age Ageing* **34**, 561–566 (2005).
9. Mollenhauer, B. Status of current biofluid biomarkers in Parkinson's disease. *Mov. Disord. Clin. Pract.* **10**, S18–S20 (2023).
10. Bentivenga, G. M. et al. Performance of a seed amplification assay for misfolded alpha-synuclein in cerebrospinal fluid and brain tissue in relation to Lewy body disease stage and pathology burden. *Acta Neuropathol.* **147**, 18 (2024).
11. Rossi, M. et al. Diagnostic value of the CSF alpha-synuclein real-time quaking-induced conversion assay at the prodromal mci stage of dementia with Lewy bodies. *Neurology* **97**, e930–e940 (2021).
12. Bellomo, G. et al. Investigating alpha-synuclein co-pathology in Alzheimer's disease by means of cerebrospinal fluid alpha-synuclein seed amplification assay. *Alzheimers Dement.* **20**, 2444–2452 (2024).
13. Collij, L. E. et al. Lewy body pathology exacerbates brain hypometabolism and cognitive decline in Alzheimer's disease. *Nat. Commun.* **15**, 8061 (2024).
14. McKeith, I. et al. Sensitivity and specificity of dopamine transporter imaging with 123I-FP-CIT SPECT in dementia with Lewy bodies: a phase III, multicentre study. *Lancet Neurol.* **6**, 305–313 (2007).
15. Benamer, T. S. et al. Accurate differentiation of parkinsonism and essential tremor using visual assessment of [123I]-FP-CIT SPECT imaging: the [123I]-FP-CIT study group. *Mov. Disord.* **15**, 503–510 (2000).
16. Del Campo, M. et al. CSF proteome profiling reveals biomarkers to discriminate dementia with Lewy bodies from Alzheimer s disease. *Nat. Commun.* **14**, 5635 (2023).
17. Pereira, J. B. et al. DOPA decarboxylase is an emerging biomarker for Parkinsonian disorders including preclinical Lewy body disease. *Nat. Aging* **3**, 1201–1209 (2023).
18. Paslawski, W. et al. Large-scale proximity extension assay reveals CSF midkine and DOPA decarboxylase as supportive diagnostic biomarkers for Parkinson's disease. *Transl. Neurodegener.* **12**, 42 (2023).
19. Rutledge, J. et al. Comprehensive proteomics of CSF, plasma, and urine identify DDC and other biomarkers of early Parkinson's disease. *Acta Neuropathol.* **147**, 52 (2024).
20. Bertoldi, M. Mammalian DOPA decarboxylase: structure, catalytic activity and inhibition. *Arch. Biochem. Biophys.* **546**, 1–7 (2014).
21. Hsam, O. & Kohl, Z. Serotonin in synucleinopathies. *Behav. Brain Res.* **445**, 114367 (2023).
22. Bolsewig, K. et al. Increased plasma DOPA decarboxylase levels in Lewy body disorders are driven by dopaminergic treatment. *Nat. Commun.* **16**, 1139 (2025).
23. Appleton, E. et al. DOPA-decarboxylase is elevated in CSF, but not plasma, in prodromal and de novo Parkinson's disease. *Transl. Neurodegener.* **13**, 31 (2024).
24. Aviolat, H., Mollon, J., Giaisi, S., Barghorn, S. & Heym, R. G. A monoclonal antibody-based immunoassay reinforces DOPA decarboxylase in cerebrospinal fluid as a diagnostic and prognostic biomarker for Parkinson's disease. Preprint at *medRxiv* https://doi.org/10.1101/2025.02.26.25322938 (2025).
25. Andreasson, U. et al. A practical guide to immunoassay method validation. *Front. Neurol.* **6**, 179 (2015).
26. Savica, R. et al. Lewy body pathology in Alzheimer's disease: a clinicopathological prospective study. *Acta Neurol. Scand.* **139**, 76–81 (2019).
27. Robinson, J. L. et al. The development and convergence of co-pathologies in Alzheimer's disease. *Brain* **144**, 953–962 (2021).
28. DeTure, M. A. & Dickson, D. W. The neuropathological diagnosis of Alzheimer's disease. *Mol. Neurodegener.* **14**, 32 (2019).
29. McFarland, N. R. Diagnostic approach to atypical Parkinsonian syndromes. *Continuum* **22**, 1117–1142 (2016).
30. Rossi, M. et al. Ultrasensitive RT-QuIC assay with high sensitivity and specificity for Lewy body-associated synucleinopathies. *Acta Neuropathol.* **140**, 49–62 (2020).
31. van Rumund, A. et al. alpha-Synuclein real-time quaking-induced conversion in the cerebrospinal fluid of uncertain cases of parkinsonism. *Ann. Neurol.* **85**, 777–781 (2019).
32. Bongianni, M. et al. alpha-Synuclein RT-QuIC assay in cerebrospinal fluid of patients with dementia with Lewy bodies. *Ann. Clin. Transl. Neurol.* **6**, 2120–2126 (2019).
33. Belujon, P. & Grace, A. A. Dopamine system dysregulation in major depressive disorders. *Int. J. Neuropsychopharmacol.* **20**, 1036–1046 (2017).
34. Khosousi, S. et al. Increased CSF DOPA decarboxylase correlates with lower DaT-SPECT binding: analyses in Biopark and PPMI cohorts. *Mov. Disord.* **39**, 1881–1885 (2024).
35. Walker, Z. et al. Striatal dopamine transporter in dementia with Lewy bodies and Parkinson disease: a comparison. *Neurology* **62**, 1568–1572 (2004).
36. Marquie, M. et al. Striatal and extrastriatal dopamine transporter levels relate to cognition in Lewy body diseases: an (11)C altropane positron emission tomography study. *Alzheimers Res. Ther.* **6**, 52 (2014).
37. Tehranian, R., Montoya, S. E., Van Laar, A. D., Hastings, T. G. & Perez, R. G. Alpha-synuclein inhibits aromatic amino acid decarboxylase activity in dopaminergic cells. *J. Neurochem.* **99**, 1188–1196 (2006).
38. Mori, F. et al. Relationship among alpha-synuclein accumulation, dopamine synthesis, and neurodegeneration in Parkinson disease substantia nigra. *J. Neuropathol. Exp. Neurol.* **65**, 808–815 (2006).
39. Catani, M., Dell'acqua, F. & Thiebaut de Schotten, M. A revised limbic system model for memory, emotion and behaviour. *Neurosci. Biobehav. Rev.* **37**, 1724–1737 (2013).
40. Harris, K. D. & Mrsic-Flogel, T. D. Cortical connectivity and sensory coding. *Nature* **503**, 51–58 (2013).
41. Hok, A. H. Y. S. et al. Thimet oligopeptidase as a potential CSF biomarker for Alzheimer's disease: a cross-platform validation study. *Alzheimers Dement.* **15**, e12456 (2023).
42. Wojdala, A. L. et al. Phosphatidylethanolamine binding protein 1 (PEBP1) in Alzheimer's disease: ELISA development and clinical validation. *J. Alzheimers Dis.* **88**, 1459–1468 (2022).
43. Hok, A. H. Y. S. et al. Neuroinflammatory CSF biomarkers MIF, sTREM1, and sTREM2 show dynamic expression profiles in Alzheimer's disease. *J. Neuroinflammation* **20**, 107 (2023).

Katharina Bolsewig[1,2] ✉, Giovanni Bellomo[3,4], Yanaika S. Hok-A-Hin[1,2], Imane Al Idrissi[1,2], Lisa Vermunt[1,2,5], Alberto Lleó[6,7], Daniel Alcolea[6,7], Anne Sieben[8,9,10], Sebastiaan Engelborghs[11,12,13], Anja Hviid Simonsen[14], Steen G. Hasselbalch[14], Sara Bech[15], Tjado H. J. Morrema[2,16], Jeroen J. M. Hoozemans[2,16], John G. J. M. Bol[2,17], Juliette van Alphen[2,5], Lorenzo Gaetani[3], Davide Chiasserini[3], Federico Paolini Paoletti[3], Lucilla Parnetti[3], Sungwoo Kang[18], Young-gun Lee[19], Suhee Jeon[20], Ahreum Lee[20], Seun Jeon[20], Byoung Seok Ye[21], Marta del Campo Milán[22,23], Wiesje M. van der Flier[2,24,25,26], Wilma D. J. van de Berg[2,17], Afina W. Lemstra[2,5], Eline A. J. Willemse[1,27] & Charlotte E. Teunissen[1,2]

[1]Neurochemistry Laboratory, Laboratory Medicine Department, Amsterdam Neuroscience, VU University Medical Centers, Amsterdam UMC, Amsterdam, the Netherlands. [2]Amsterdam Neuroscience, Neurodegeneration program, Amsterdam UMC, Amsterdam, the Netherlands. [3]Department of Medicine and Surgery, Section of Neurology, University of Perugia, Perugia, Italy. [4]Department of Life Science, Health, and Health Professions, Link Campus University, Rome, Italy. [5]Amsterdam Alzheimer Center, Amsterdam University Medical Centers, Amsterdam, the Netherlands. [6]Department of Neurology, Institut d'Investigacions Biomèdiques Sant Pau (IIB SANT PAU) - Hospital de Sant Pau, Universitat Autònoma de Barcelona, Hospital de la Santa Creu i Sant Pau, Barcelona, Spain. [7]Center of Biomedical Investigation Network for Neurodegenerative Diseases (CIBERNED), Madrid, Spain. [8]Neuropathology lab, IBB-NeuroBiobank BB1901113, Born Bunge Institute, Antwerp, Belgium. [9]Department of Pathology, Antwerp University Hospital - UZA, Antwerp, Belgium. [10]Laboratory of Neurology, Translational Neurosciences, Faculty of Medicine and Health Sciences, University of Antwerp, Antwerp, Belgium. [11]Reference Center for Biological Markers of Dementia (BIODEM), Laboratory of Neurochemistry and Behavior, Institute Born-Bunge, University of Antwerp, Antwerp, Belgium. [12]Vrije Universiteit Brussel, Center for Neurosciences (C4N), Neuroprotection and Neuromodulation Research Group (NEUR), Brussels, Belgium. [13]Department of Neurology, Universitair Ziekenhuis Brussel, Brussels, Belgium. [14]Danish Dementia Research Centre, Rigshospitalet, University of Copenhagen, Copenhagen, Denmark. [15]Department of Neurology, Bispebjerg and Frederiksberg Hospital, Copenhagen University Hospital, Copenhagen, Denmark. [16]Amsterdam UMC, Department of Pathology, Amsterdam Neuroscience, Amsterdam, the Netherlands. [17]Department of Anatomy and Neurosciences, Section Clinical Neuroanatomy and Biobanking, Amsterdam UMC, Vrije University, Amsterdam, the Netherlands. [18]Department of Neurology, Hanyang Seoul Hospital, Hanyang University College of Medicine, Seoul, Republic of Korea. [19]Department of Neurology, Ilsan Paik Hospital, Inje University College of Medicine, Goyang, Republic of Korea. [20]Metabolism-Dementia Research Institute, Yonsei University College of Medicine, Seoul, Republic of Korea. [21]Department of Neurology, Yonsei University College of Medicine, Seoul, Republic of Korea. [22]BarcelonaBeta Brain Research Center, Pasqual Maragall Foundation, Barcelona, Spain. [23]Hospital del Mar Research Institute (IMIM), Barcelona, Spain. [24]Epidemiology and Data Science, Vrije Universiteit Amsterdam, Amsterdam UMC location VUmc, Amsterdam, the Netherlands. [25]Alzheimer Nederland, Amersfoort, the Netherlands. [26]Amsterdam Public Health, Amsterdam, the Netherlands. [27]Department of Neurology, Multiple Sclerosis Center and Research Center for Clinical Neuroimmunology and Neuroscience Basel, Departments of Biomedicine and Clinical Research, University Hospital Basel and University of Basel, Basel, Switzerland. ✉e-mail: k.bolsewig@amsterdamumc.nl

Methods

Inclusion and ethics

Informed written consent was given by all participants or their legal representatives, for their medical data and biomaterials to be used for scientific research. The study was conducted in accordance with the Declaration of Helsinki[44] and was approved by the local ethical committees of each participating center (ADC: AD CSF biobank METC no. 2017.315, SPIN: COLLECTION 16/2013, DDBB/BMDB Validation: H-23001553, UNIPG αS-SAA: Comitato Etico Aziende Sanitarie Regione Umbria 19369/AV and 20942/21/OV, BIODEM/UAntwerp Autopsy: EC of ZNA (approval no. 4363) and EC UZA / UAntwerp (14/12/130), YUHS DaT-PET: review board of Severance Hospital (IRB No. 4-2018-0944 and IRB No. 4-2024-0877)).

Immunoassay development and optimization

Immunoassay development was performed on the SimplePlex Ella platform (ProteinSimple) in CSF and the Quanterix Simoa platform (Quanterix) in CSF, plasma and serum. Both assays are based on a sandwich ELISA setup and were optimized for customizable assay parameters, that is, antibody combinations and concentrations, buffer conditions, sample dilution and volume. The Simoa assay was additionally optimized for addition of helper beads, incubation steps and times, and substrate concentration. A more detailed description of the assay optimization steps is given in Supplementary Methods 1.

Analytical validation

Analytical validations of the in-house-developed immunoassays were performed according to consensus guidelines[25]. Both assays were validated for lower limit of detection, precision, parallelism, dilution linearity, recovery and sample stability for the use in CSF (Supplementary Methods 2), and the Simoa assay was additionally validated for the use in plasma and serum (Supplementary Methods 3). Coefficients of variations of <20% were considered acceptable, and for parallelism, dilution linearity, recovery and sample stability, the accepted range of deviation of the samples from the reference condition was 85% to 115%.

Study population

We included participants from six different cohorts: ADC[16] Discovery (CTRL, $n = 50$; DLB, $n = 41$; AD, $n = 51$), a clinical multicenter validation cohort from the ADC and SPIN[45] (ADC/SPIN Validation; CTRL, $n = 108$; DLB; $n = 106$; MCI-A+, $n = 101$; AD dementia, $n = 104$), a DLB/PD cohort from the DDBB/BMDB (DDBB/BMDB Validation; CTRL, $n = 44$; DLB, $n = 46$; PD, $n = 37$; AD; $n = 52$), a biologically confirmed cohort from the University of Perugia, which consisted of participants with αS-SAA measurements previously performed with the 24-h Amprion protocol[12] (UNIPG αS-SAA; CTRL (negative αS-SAA), $n = 65$; AD continuum, $n = 110$ (MCI-AD, $n = 61$; pre-AD, $n = 11$; AD dementia, $n = 38$); PD + DLB, $n = 78$ (all αS-SAA positive; cognitively normal PD, $n = 33$; PD-MCI, $n = 34$; PDD/DLB, $n = 11$)), an autopsy-confirmed cohort from the Reference Center for Biological Markers of Dementia (BIODEM) and the neurobiobank of the Institute Born-Bunge of the University of Antwerp (BIODEM/UAntwerp Autopsy; CTRL, $n = 30$; pathologically confirmed DLB, $n = 18$; pathologically confirmed AD, $n = 30$) and a cohort with detailed DaT-PET imaging data from the Yonsei University Health System of which $n = 90$ (88.2%) presented with significant parkinsonism (YUHS DaT-PET; total, $n = 102$, DaT-PET normal/abnormal, $n = 24/78$), which did not include healthy controls. Of note, the ADC Discovery Cohort, ADC/SPIN Validation Cohort and the BIODEM/UAntwerp Autopsy Cohort were also included in our previous proteomics study[16].

AD core CSF biomarkers ($A\beta_{42}$ or $A\beta4_{2/40}$, pTau181 and tTau) were used to support the clinical diagnosis of AD (abnormal $A\beta_{42}$ or $A\beta_{42/40}$ ratio and abnormal pTau181) and to confirm underlying amyloid pathology in the MCI group (as defined by abnormal $A\beta_{42}$ or $A\beta_{42/40}$ ratio) in the ADC Discovery, ADC/SPIN Validation and DDBB/BMDB Validation. In the UNIPG αS-SAA, AD was defined based on abnormal $A\beta_{42/40}$ ratio and abnormal pTau181 (ref. 46) and in the YUHS DaT-PET AD was defined based on cerebral amyloid deposition measured by Florbetaben PET[47]. These markers were measured at each center with commercially available assays (ELISA INNOTEST $A\beta_{1-42}$, hTAUAg, phospho-Tau(181 P) (Fujirebio-Europe): ADC, BIODEM-IBB/University of Antwerp, Danish Dementia Biobank; $A\beta_{1-42}$, total-Tau, phospho-Tau181 Elecsys biomarker assays (Roche Diagnostics): ADC; Lumipulse G600 (Fujirebio-Europe): SPIN, University of Perugia). To determine biomarker abnormality, lab-specific cutoff values were applied (ADC[48,49]: $A\beta_{42Innotest} < 813$ pg ml^{-1}, $pTau_{Innotest} > 52$ pg ml^{-1}, $tTau_{Innotest} > 375$ pg ml^{-1} or $A\beta_{42Elecsys} < 1{,}000$ pg ml^{-1}, $pTau_{Elecsys} > 19$ pg ml^{-1}, $tTau_{Elecsys} > 235$ pg ml^{-1}; SPIN[50]: $A\beta_{42/40Lumipulse} < 0.062$, $pTau_{Lumipulse} > 63$ pg ml^{-1}, $tTau_{Lumipulse} > 456$ pg ml^{-1}; BIODEM/U Antwerp[51]: $A\beta_{42Innotest} < 638.5$ pg ml^{-1}, $pTau_{Innotest} > 56.5$ pg ml^{-1}, $tTau_{Innotest} > 296.5$ pg ml^{-1}; Danish Dementia Biobank[52]: $A\beta_{42Innotest} < 400$ pg ml^{-1} (for measurements before 2013), <550 pg ml^{-1} (for measurements 2013–2018) or $A\beta_{42Innotest} < 1{,}016$ pg ml^{-1} (for measurements between 2018 and July 2022), or $A\beta_{42Elecsys} < 1{,}030$ pg ml^{-1} (for measurements after July 2022), $pTau_{Innotest} > 60$ pg ml^{-1} (for patients younger than 60 years old) or >80 pg ml^{-1} (for patients older than 60 years old) before 2022 or $pTau_{Elecsys} > 25$ pg ml^{-1} from 2022 onward, $tTau_{Innotest} > 400$ pg ml^{-1} before 2022 or $tTau_{Elecsys} > 250$ pg ml^{-1} from 2022 onward; University of Perugia[53]: $A\beta_{42/40Lumipulse} < 0.072$, $pTau_{Lumipulse} > 50$ pg ml^{-1}, $tTau_{Lumipulse} > 392$ pg ml^{-1}). AD CSF biomarker measurements were available for subsets of the patients with DLB and PD: ADC Discovery, $n = 38$; ADC/SPIN Validation, $n = 106$; DDBB/BMDB Validation (PD), $n = 14$, DDBB/BMDB Validation (DLB), $n = 32$; UNIPG αS-SAA (CSF Ella), $n = 55$; UNIPG αS-SAA (CSF Simoa) $A\beta_{42/40}$, $n = 73$; pTau and tTau, $n = 75$; UNIPG αS-SAA (Plasma Simoa) $A\beta_{42/40}$, $n = 50$; pTau and tTau, $n = 52$; BIODEM/UAntwerp Autopsy, $n = 13$. In the YUHS DaT-PET, AD CSF biomarkers were available for all patients.

Information on DaT-Scan status was available for subsets of patients with DLB and PD; ADC Discovery (n DaT-Scan performed = 6), ADC/SPIN Validation (n DaT-Scan performed = 48) and DDBB/BMDB Validation (n DaT-Scan performed in DLB = 7; n DaT-Scan performed in PD = 19). Abnormal DaT-Scan could support the clinical diagnoses of 50/61 patients with DLB and 19/19 patients with PD. All patients in the YUHS DaT-PET underwent DaT-PET imaging (Supplementary Methods 4). Information on presence of DLB core features was available for subsets of the DLB group in ADC Discovery and ADC/SPIN Validation (Extended Data Table 6).

In all cohorts, participants underwent standard neurological and cognitive assessments and patients with DLB, PD, mild cognitive impairment and AD were diagnosed according to the respective diagnostic criteria[6,7,46,54,55], or were defined according to international neuropathological examination guidelines for AD[56] and DLB[7,57] (BIODEM/UAntwerp Autopsy). Additionally, all patients with PD + DLB from the UNIPG αS-SAA, had positive CSF αS-SAA. Approximately 50% of the patients with AD in the UNIPG αS-SAA had positive CSF αS-SAA. Diagnoses in the YUHS DaT-PET were made based on clinical examination, neurological examination, AD CSF biomarkers and brain magnetic resonance imaging and included one or more etiologies for cognitive decline including AD, DLB, normal pressure hydrocephalus, vascular cognitive impairment, progressive supranuclear palsy and semantic variant primary progressive aphasia. Patients who exhibited parkinsonism or mild fluctuations and visual hallucinations that were not sufficient to be classified as DLB were categorized as possible LBD (pLBD). Controls in ADC Discovery and ADC/SPIN Validation were participants with subjective cognitive decline who did not present with any cognitive abnormalities during the diagnostic workup (ADC), or volunteers with normal neuropsychological scores (SPIN[45]). Controls in the DDBB/BMDB Validation were cognitively healthy individuals who were referred to diagnostic evaluation at the Danish Dementia Research Centre's memory clinic but who were found without dementia or MCI. Controls of the UNIPG αS-SAA were cognitively normal

individuals ($n = 32$) or individuals with MCI who had a normal AD CSF biomarker profile ($n = 33$) and negative CSF αS-SAA. Controls in the BIODEM/UAntwerp Autopsy were not pathologically confirmed and consisted of volunteers without any neurological or psychiatric diseases and did not present with any cognitive abnormalities[58]. Demographic characteristics of the included fluid cohorts are summarized in Extended Data Tables 1–3.

Immunohistochemistry was performed in postmortem brainstem tissue from pathology-confirmed controls ($n = 4$), patients with DLB ($n = 4$) and patients with PD(D) ($n = 4$). Brain tissue from patients with DLB and PD(D) was acquired from the Netherlands Brain Bank (http://brainbank.nl/) or from controls through the Normal Aging Brain Collection Amsterdam (http://nabca.eu/). The neuropathological diagnoses were established according to international guidelines of the Brain Net Europe II consortium (http://www.brainnet-europe.org/)[56,59,60]. Demographics and neuropathological characteristics of these donors are listed in Extended Data Table 8.

DDC measurements

DDC in CSF was measured with the in-house Ella and Simoa assays described above. In short, for measurements on the Ella system, 50 µl of CSF was measured in a twofold dilution. Inherent to the Ella technology, each sample was measured in triplicate. For measurements on the Simoa system, 100 µl of CSF were measured in a sixfold dilution. Each sample was measured in duplicate. For both assays, DDC concentrations were calculated with a four-parameter logistic curve, describing a calibration curve of recombinant human DDC. DDC concentrations in CSF were measured with our in-house-developed immunoassays in six different cohorts. DDC measurements on the Ella platform were performed in the ADC Discovery, ADC/SPIN Validation, BIODEM/UAntwerp Autopsy and UNIPG αS-SAA, and measurements on the Simoa platform were performed in the ADC Discovery, DDBB/BMDB Validation, UNIPG αS-SAA and YUHS DaT-PET. Ella measurements in the ADC/SPIN Validation were performed on Ella V4 cartridges, while the ADC Discovery, BIODEM/UAntwerp Autopsy and UNIPG αS-SAA were measured on the updated Ella V5 cartridges. We performed a Passing Bablok regression based on 50 samples from the ADC/SPIN Validation and identified that levels on the Ella V5 cartridges were about 10 pg ml^{-1} higher compared to measurements on the Ella V4 cartridges. The Passing Bablok regression resulted in the conversion formula as shown in equation (1):

$$\mathrm{EllaV5} = 9.64 + 1.02 \times \mathrm{EllaV4} \quad (1)$$

This conversion formula has been applied to ADC/SPIN Validation before analysis to allow comparability between cohorts.

Additionally, PEA measurements of DDC in CSF were available for the ADC, SPIN and BIODEM/UAntwerp Autopsy from our previous study[16].

Detection of DDC with immunohistochemistry

For DDC single stainings, 6-µm-thick formalin-fixed and paraffin embedded tissue sections from the brainstem, including the substantia nigra (at the level of the midbrain) and raphe nucleus (at the rostral level of the pons), were first deparaffinized using a xylene substitute and rehydrated in a series of ethanol with decreasing alcohol percentages. Next, antigen retrieval was performed for 30 min in citrate buffer (pH 6.0) in a steam cooker. Sections were washed in Tris-buffered saline (TBS) and incubated in TBS with 1% hydrogen peroxide (H_2O_2) for 30 min at room temperature to block endogenous peroxidase activity. Afterward, sections were washed with TBS at room temperature. To prevent nonspecific binding of the primary antibody, sections were blocked in TBS with 5% of elk milk powder and 0.1% Triton X-100 for 30 min. Subsequently, sections were incubated with primary anti-DDC antibody (1:400 dilution; AF3564, R&D Systems, detection antibody from DDC Ella and Simoa immunoassays), diluted in TBS overnight at 4 °C. The following day, sections were washed with TBS at room temperature and incubated for 30 min with ImmPRESS horse anti-goat antibody, coupled to horseradish peroxidase (HRP; MP-7405, Vector). After washing with TBS-HCl, Vector SG (SK-4700, Vector) was applied to the sections as chromogen for 25 min. Lastly, sections were dehydrated and mounted using Entellan.

Triple labeling experiments were performed for DDC, tyrosine hydroxylase and phosphorylated Ser129 α-syn on 6-µm-thick formalin-fixed and paraffin embedded sections from the substantia nigra. After deparaffinization and antigen retrieval as described above, sections were subsequently incubated in a blocking buffer containing 3% normal donkey serum and 0.1% Triton X in TBS for 30 min. Afterward, sections were incubated with primary anti-tyrosine hydroxylase antibody (MAB318, 1:200 dilution, Chemicon) overnight at 4 °C. The following day, sections were washed and incubated for 30 min at room temperature with the Envision system, containing secondary anti-mouse antibody, coupled to HRP (K400111-2, Dako). Subsequently, sections were washed in Tris-HCl and labeled with Tyramid Alexa Fluor 568 (B40956, 1:100 dilution, Thermo Fisher Scientific) in Tris-HCl + 0.005% H_2O_2 for 20 min. After the sections were washed in TBS and the antigen retrieval and blocking were repeated, sections were incubated with primary phosphorylated Ser129 α-syn (EP1536Y, 1:300 dilution, Abcam) and DDC (1:100 dilution, AF3564, R&D Systems) antibodies for 48 h at 4 °C. The following day, the sections were washed with TBS and incubated with Alexa Fluor 647-labeled donkey anti rabbit (A-31573, 1:400 dilution, Thermo Fisher Scientific) and DAPI (1:1,000 dilution, Thermo Fisher Scientific) for 2 h at room temperature. Sections were washed with TBS and incubated with ImmPRESS horse anti-goat antibody, coupled to HRP (MP-7405, Vector) for 30 min at room temperature, then washed with Tris-HCl and labeled with Tyramid Alexa Fluor 488 (B40953, 1:100 dilution, Thermo Fisher Scientific) in Tris-HCl with 0.005% H_2O_2 for 20 min, and subsequently washed in TBS. Sections were mounted in Mowiol mounting solution (Sigma-Aldrich) using glass coverslips. Negative control stainings lacking primary antibodies were performed to control for background/autofluorescence levels and unspecific staining. Single labeling for each antibody included in multiple-labeling experiments were carefully examined to control whether immunoreactivity patterns were caused by possible cross-reactivity between antibodies.

Brightfield and confocal laser scanning microscopy

The immunostained sections were first examined qualitatively by means of light microscopy (Leica DM5000 B photo microscope). High-resolution images were captured with the Leica DFC450 camera (HC PL APO ×20 1.30-NA oil or HC PL APO ×63 1.40-NA 0.60 oil objective) and the LAS 4.0 software. Neuromelanin-positive neurons in the substantia nigra of sections immunostained for phosphorylated α-syn/TH/DDC/DAPI were imaged using the Leica TCS SP8 STED ×3 confocal laser scanning microscope (CSLM: Leica Microsystems). All images were acquired using a HC PL APO CS2 ×100 1.4-NA oil objective lens, with the resolution set to a pixel size of 20 nm × 20 nm. Gated hybrid detectors were used in counting mode. Sections were sequentially scanned for each fluorophore, by irradiation with a pulsed white light laser at different wavelengths. Images were taken as *z*-stacks to allow deconvolution and three-dimensional image analysis (0.6 µm *z*-stack, 0.15 µm *z*-steps). Autofluorescence in the 488-nm and 594-nm channels was measured and extracted from the images, and compared to sections stained without primary antibodies (negative controls) to assess background signal. Deconvolution on the image stacks was performed using the Huygens Professional software package (Scientific Volume Imaging), using the manufacturer-recommended settings and the Batch Processor to apply the same settings to all images. Images were adjusted for brightness/contrast in the same way using an ImageJ (National Institute of Health).

Statistics and reproducibility

All statistical analyses were performed with R Studio (version 4.0.5)[61]. Distribution of data was analyzed by visual examination and Shapiro–Wilk test (pastecs R package[62], version 1.4.2). To achieve a normal distribution, DDC, Aβ42, pTau and tTau concentrations were $\log_{10}$-transformed, and MMSE scores were subtracted from 31 and subsequently $\log_{10}$-transformed. Differences of DDC concentrations across diagnostic groups were assessed by ANCOVA (car R package[63], version 3.1.2), corrected for age and sex (and center in ADC/SPIN Validation) with Tukey's post hoc test. The potential of DDC to separate DLB from the other diagnostic groups was determined through ROC analysis (pROC R package[64], version 1.18.5). First, we performed a ROC analysis for a basic model including only age and sex as predictors, or models including only DDC as predictor (DDC only) and next evaluated the added value of DDC to the basic models. Cutoff values were calculated from uncorrected and untransformed CSF DDC concentrations based on the Youden index. Meta-analyses of SMDs of DDC levels were performed between DLB and PD and other diagnostic groups (meta R package[65], version 8.0.1). In cohorts that were measured with the Ella assay only, measurements were transformed to Simoa measurements beforehand. Association of DDC levels with cognitive impairment was analyzed by linear regression corrected for age and sex (and center in ADC/SPIN Validation). In the DLB group, associations between DDC levels and presence of DLB core features and AD CSF biomarker status were assessed through ANCOVA, corrected for age and sex (and center in ADC/SPIN Validation). Association of CSF DDC levels with motor impairment was assessed in the PD + DLB group in the UNIPG αS-SAA and in the YUHS DaT-PET by linear regression corrected for age, sex, LEDD and disease duration. Association between CSF DDC and DaT-PET in the caudate and putamen was analyzed by linear regression corrected for age, sex and education in the YUHS DaT-PET, and corrected for multiple testing by applying false discovery rate correction using the Benjamini–Hochberg procedure with a significance threshold of $q < 0.05$. Lastly, correlations between DDC measurements by PEA and by our in-house-developed immunoassays were analyzed with Spearman's correlation. To evaluate the relation between the developed Ella and Simoa assays, as well as Ella V4 and Ella V5 cartridge format, we performed a Passing Bablok regression (mcr R package[66], version 1.3.3). All statistical tests were two tailed, and a significance level of $\alpha = 0.05$ was accepted.

Reporting summary

Further information on research design is available in the Nature Portfolio Reporting Summary linked to this article.

Data availability

Requests for raw data can be sent to the corresponding author (K.B.) and will be reviewed by the research team from the Amsterdam UMC, typically within 2 weeks. Upon positive evaluation without obligations regarding intellectual property or confidentiality, data will be shared through Data Transfer Agreements. Source data are provided with this paper.

References

44. World Medical Association World Medical Association Declaration of Helsinki: ethical principles for medical research involving human subjects. *JAMA* **310**, 2191–2194 (2013).
45. Alcolea, D. et al. The Sant Pau Initiative on Neurodegeneration (SPIN) cohort: a data set for biomarker discovery and validation in neurodegenerative disorders. *Alzheimers Dement.* **5**, 597–609 (2019).
46. Jack, C. R. Jr. et al. NIA-AA Research Framework: toward a biological definition of Alzheimer's disease. *Alzheimers Dement.* **14**, 535–562 (2018).
47. Lee, Y. G. et al. Amyloid-β-related and unrelated cortical thinning in dementia with Lewy bodies. *Neurobiol. Aging* **72**, 32–39 (2018).
48. Mulder, C. et al. Amyloid-beta(1–42), total tau, and phosphorylated tau as cerebrospinal fluid biomarkers for the diagnosis of Alzheimer disease. *Clin. Chem.* **56**, 248–253 (2010).
49. Tijms, B. M. et al. Unbiased approach to counteract upward drift in cerebrospinal fluid amyloid-beta 1–42 analysis results. *Clin. Chem.* **64**, 576–585 (2018).
50. Alcolea, D. et al. Agreement of amyloid PET and CSF biomarkers for Alzheimer's disease on Lumipulse. *Ann. Clin. Transl. Neurol.* **6**, 1815–1824 (2019).
51. Somers, C. et al. A decade of cerebrospinal fluid biomarkers for Alzheimer's disease in Belgium. *J. Alzheimers Dis.* **54**, 383–395 (2016).
52. Simonsen, A. H., Musaeus, C. S., Christensen, G. L., Hasselbalch, S. G. & Waldemar, G. Upwards drift of cerebrospinal fluid amyloid-beta 42 over twelve years in a consecutive clinical cohort. *J. Alzheimers Dis.* **81**, 1369–1373 (2021).
53. Bellomo, G. et al. Machine learning driven profiling of cerebrospinal fluid core biomarkers in Alzheimer's disease and other neurological disorders. *Front. Neurosci.* **15**, 647783 (2021).
54. Albert, M. S. et al. The diagnosis of mild cognitive impairment due to Alzheimer's disease: recommendations from the National Institute on Aging-Alzheimer's Association workgroups on diagnostic guidelines for Alzheimer's disease. *Alzheimers Dement.* **7**, 270–279 (2011).
55. McKhann, G. M. et al. The diagnosis of dementia due to Alzheimer's disease: recommendations from the National Institute on Aging-Alzheimer's Association workgroups on diagnostic guidelines for Alzheimer's disease. *Alzheimers Dement.* **7**, 263–269 (2011).
56. Montine, T. J. et al. National Institute on Aging-Alzheimer's Association guidelines for the neuropathologic assessment of Alzheimer's disease: a practical approach. *Acta Neuropathol.* **123**, 1–11 (2012).
57. McKeith, I. G. et al. Diagnosis and management of dementia with Lewy bodies: third report of the DLB Consortium. *Neurology* **65**, 1863–1872 (2005).
58. Ottoy, J. et al. Association of short-term cognitive decline and MCI-to-AD dementia conversion with CSF, MRI, amyloid- and (18) F-FDG-PET imaging. *Neuroimage Clin.* **22**, 101771 (2019).
59. Alafuzoff, I. et al. Staging of neurofibrillary pathology in Alzheimer's disease: a study of the BrainNet Europe Consortium. *Brain Pathol.* **18**, 484–496 (2008).
60. Alafuzoff, I. et al. Staging/typing of Lewy body related alpha-synuclein pathology: a study of the BrainNet Europe Consortium. *Acta Neuropathol.* **117**, 635–652 (2009).
61. R Core Team. R: a language and environment for statistical computing. R Foundation for Statistical Computing: Vienna, Austria https://www.R-project.org/ (2020).
62. Grosjean, P. & Ibanez, F. pastecs: package for analysis of space-time ecological series. R package version 1.3 (2018).
63. Fox, J. & Weisberg, S. *An R Companion to Applied Regression* (Sage, 2019).
64. Robin, X. et al. pROC: an open-source package for R and S+ to analyze and compare ROC curves. *BMC Bioinformatics* **12**, 77 (2011).
65. Balduzzi, S., Rucker, G. & Schwarzer, G. How to perform a meta-analysis with R: a practical tutorial. *Evid. Based Ment. Health* **22**, 153–160 (2019).
66. Potapov, S. et al. MCR: method comparison regression. https://CRAN.R-project.org/package=mcr/ (2023).

Acknowledgements

This project has received funding from the European Union's Horizon 2020 research and innovation program under the Marie Skłodowska-Curie grant agreement no. 860197, 'MIRIADE' (to K.B., C.E.T. and E.A.J.W.).

Y.S.H. is funded with PPP-allowance from Health~Holland. G.B. was supported by the Postdoctoral Fellowship for Basic Scientists grant of the Parkinson's Foundation (award ID: PF-PRF-934916). The SPIN cohort received funding from the Fondo de Investigaciones Sanitario (FIS), Instituto de Salud Carlos III (PI22/00307, PI21/00791, PI14/01126, PI17/01019, PI20/01473, PI13/01532, PI16/01825, PI18/00335, PI19/00882, PI18/00435, PI22/00611, INT19/00016, INT23/00048, PI17/01896 and AC19/00103) and the CIBERNED program (Program 1, Alzheimer Disease to A.L.), jointly funded by Fondo Europeo de Desarrollo Regional, Unión Europea, "Una manera de hacer Europa". L.P. and L.G. were funded by the European Union—Next Generation EU – PNRR M6C2 - Investimento 2.1 Valorizzazione e potenziamento della ricerca biomedica del SSN (PNRR-MAD-2022-12376035). L.G. was supported by the Young Researcher grant (AGYR 2023) of the AirAlzh (Associazione Italiana Ricerca Alzheimer Onlus). B.S.Y. was supported by the National Research Foundation of Korea grant funded by the Korea government (MSIT; no. RS-2025-18362970) and by a grant of the Korea Health Technology R&D Project through the Korea Health Industry Development Institute (KHIDI), funded by the Ministry of Health & Welfare, Republic of Korea (HR22C141101). M.d.C.M. receives support from Ramon y Cajal fellowship (RYC2023-043831-I funded by MCIN/AEI/10.13039/501100011033 and the FSE+), MCIN/AEI/10.13039/501100011033/FEDER, EU, through the project (PID2023-153312OB-I00) and Caixa Research Institute. W.M.v.d.F. was recipient of TAP-dementia (www.tap-dementia.nl/), receiving funding from ZonMw (10510032120003). W.D.J.v.d.B. was supported by a grant from the Stichting Woelse Waard (ParKCODE). The research of C.E.T. is supported by the European Commission (MarieCurie International Training Network, grant agreement nos. 860197 (MIRIADE) and 101119596 (TAME), Innovative Medicines Initia-tives 3TR (Horizon 2020, grant 831434), EPND (IMI 2 Joint Under-taking (JU), grant 101034344) and JPND (bPRIDE, CCAD), EuropeanPartnership on Metrology, co-financed by the European Union's Horizon Europe Research and Innovation Programme and by the Participating States (22HLT07 NEuroBioStand), Horizon Europe (PREDICTFTD, 101156175, CCAD), CANTATE project funded by the Alzheimer's Drug Discovery Foundation, Alzheimer's Association (grant SG-22-856131-SABB NEXT), Michael J. Fox Foundation, Health Holland, the Dutch Research Council (ZonMW), Alzheimer's Drug Discovery Foundation, Selfridges Group Foundation and Alzheimer Netherlands. C.E.T. is recipient of ABOARD, which is a public–private partnership receiving funding from ZonMW (no. 73305095007) and Health~Holland, Topsector Life Sciences & Health (PPP-allowance; no. LSHM20106). C.E.T. is recipient of TAP-dementia, a ZonMw funded project (no. 10510032120003) in the context of the Dutch National Dementia Strategy.

Author contributions

K.B.: designed study, data acquisition, performed analysis, drafted paper. G.B.: data acquisition, revised paper. Y.S.H.: data acquisition, revised paper. I.A.I.: performed laboratory work for Simoa assay, revised paper. L.V.: data acquisition, revised paper. A. Lleó: data acquisition, revised paper. D.A.: data acquisition, revised paper. A.S.: data acquisition, revised paper. S.E.: data acquisition, revised paper. A.H.S.: data acquisition, revised paper. S.G.H.: data acquisition, revised paper. S.B.: data acquisition, revised paper. T.H.J.M.: performed stainings, revised paper. J.J.M.H.: supervised stainings, revised paper. J.G.J.M.B.: performed stainings analysis, revised paper. J.v.A.: data acquisition, revised paper. L.G.: data acquisition, revised paper. D.C.: data acquisition, revised paper. F.P.P.: data acquisition, revised paper. L.P.: data acquisition, revised paper. S.K.: data acquisition, revised paper. Y.-g.L.: data acquisition, revised paper. Suhee Jeon: data acquisition, revised paper. A. Lee.: data acquisition, revised paper. Seun Jeon: data acquisition and analysis, revised paper. B.S.Y.: data acquisition and analysis, revised paper. M.d.C.M.: data acquisition, revised paper. W.M.v.d.F.: data acquisition, revised paper. W.D.J.v.d.B.: supervised stainings analysis, drafted stainings section, revised paper. A.W.L.: data acquisition, revised paper. E.A.J.W.: supervised analysis and writing of paper, revised paper. C.E.T.: designed study, supervised writing of paper, revised paper. All authors read, revised and approved the final version of the paper.

Competing interests

K.B. received a one-time consulting fee from Fujirebio paid to the institution in 2025. G.B. received honoraria from Fujirebio and completed paid consultancies for Parkinson's Foundation. G.B. received travel/educational grants from Fujirebio and Alzheimer's Association. A. Lleó has received fees for advisory board meetings from Biogen, Beckman Coulter, Eisai, Fujirebio-Europe, Grifols, Lilly, Novartis, Roche, Otsuka Pharmaceutical, Nutricia, Zambón and Novo Nordisk. A. Lleó has received speaker honoraria from Lilly, Biogen, KRKA, Novo Nordisk, Nutricia and Zambon. A. Lleó is inventor of a patent on markers of synaptopathy in neurodegenerative disease (WO2019175379A1, Licensed to ADx) and on a patent antibody for amyloid precursor, methods and uses thereof (European priority N°EP25382226: priority date 12 Mar 2025). D.A. participated in advisory boards from Fujirebio-Europe, Roche Diagnostics, Grifols S.A. and Lilly, and received speaker honoraria from Fujirebio-Europe, Roche Diagnostics, Nutricia, Krka Farmacéutica S.L., Zambon S.A.U., Neuraxpharm, Alter Medica, Lilly and Esteve Pharmaceuticals S.A. S.E. has received consulting fees from Biogen (paid to institution), Eisai (paid to institution), Icometrix (paid to institution), Janssen (paid to institution), Eli Lilly, Novartis (paid to institution) and Remynd (paid to institution). S.E. holds patent EP3452830B1 for an assay for the diagnosis of a neurological disease (licensed to ADx Neurosciences NV & Euroimmun Medizinische Labordiagnostika AG). S.E. is a member of SMB/SAB for EU-H2020 project RECAGE and of the DSMB of PRImus-AD. A.H.S. received a one-time consulting fee from EISAI/BioArctic paid to the institution in 2025. As of 01 Jul 2024, J.J.M.H. is employed by F. Hoffmann-La Roche. Before 01 Jul 2024, J.J.M.H. received grants from the Dutch Research Council (ZonMW) and Alzheimer Netherlands, performed contract research, or received grants from Merck, ONO Pharmaceuticals, Janssen Prevention Center, Discoveric Bio, Axon Neurosciences, Roche, Genentech, Promis, Denali, FirstBiotherapeutics and Ensol Biosciences. All payments were made to the institution. J.J.M.H. participated in the scientific advisory board of Alzheimer Netherlands and has been editor-in-chief for Acta Neuropathologica Communications. L.G. has participated in advisory boards for, and received writing or speaker honoraria and travel grants from, Almirall, Biogen, Eisai, Euroimmun, Fujirebio, Lilly, Merck, Mylan, Novartis, Roche, Sanofi, Siemens Healthineers and Teva. D.C. has received travel/educational grants from Fujirebio. L.P. served as Member of Advisory Boards for Fujirebio, IBL, Roche and Merck. M.d.C.M. has been an invited speaker at Eisai and Novo Nordisk and has been an invited writer for Springer Healthcare. M.d.C.M. is an associate editor at Alzheimer´s Research & Therapy and scientific advisor for the Michael J Fox Foundation. As of 01 Nov 2025, W.M.v.d.F. is executive director at Alzheimer Nederland, Amersfoort the Netherlands. Before 01 Nov 2025, research programs of W.M.v.d.F. have been funded by ZonMW, NWO, EU-JPND, EU-IHI, Alzheimer Nederland, Hersenstichting CardioVascular Onderzoek Nederland, Health~Holland, Topsector Life Sciences & Health, Stichting Dioraphte, Noaber foundation, Pieter Houbolt Fonds, Gieskes-Strijbis fonds, Stichting Equilibrio, Edwin Bouw fonds, Pasman Stichting, Philips, Biogen MA, Novartis-NL, Life-MI, AVID, Roche BV, Eli Lilly-NL, Fujifilm, Eisai and Combinostics. W.M.v.d.F. is a recipient of ABOARD, which is a public–private partnership receiving funding from ZonMW (73305095007) and Health~Holland, Topsector Life Sciences & Health (PPP-allowance; LSHM20106). Before 01 Nov 2025, W.M.v.d.F. has been an invited speaker at Biogen MA, Danone, Eisai, WebMD Neurology (Medscape), Novo Nordisk, Springer Healthcare and the European

Brain Council. W.M.v.d.F. has been consultant to Oxford Health Policy Forum CIC, Roche, Biogen MA, Eisai, Eli Lilly, Owkin France and Nationale Nederlanden Ventures. W.M.v.d.F. has participated in advisory boards of Biogen MA, Roche and Eli Lilly. All funding has been paid to Amsterdam UMC. In 2024–2025, W.M.v.d.F. has been a member of the steering committee of phase 3 EVOKE/EVOKE+ studies (Novo Nordisk). In 2025, W.M.v.d.F. has been a member of the steering committee of a phase 3 trontinemab study (Roche). All funding has been paid to Amsterdam UMC. W.M.v.d.F. was associate editor of Alzheimer, Research & Therapy in 2020/2021. W.M.v.d.F. was associate editor at Brain 2021–2025. W.M.v.d.F. is chair of the Scientific Leadership Group of InRAD. W.M.v.d.F. is a member of the Supervisory Board (Raad van Toezicht) at Trimbos Instituut. W.D.J.v.d.B. was financially supported by grants from the Dutch Research council (ZonMW 70-73305-98-106; 70-73305-98-102), Alzheimer association (AARF-18-566459), The Michael J. Fox foundation (MJFF-022468; MJFF027187), Parkinson Association (2020-G01), Stichting Woelse Waard (ParKCODE; Nederlands Parkinson Cohort), Horizon Europe (NEUROCOV) and Parkinson Foundation (PF-TRAIL-144386). W.D.J.v.d.B. co-leads 'ProPARK', a public–private partnership receiving funding from ZonMW (40-46000-98-101), Hersenstichting, Parkinson Vereniging, PHARMO Institute NV, Stichting Woelse Waard, Stichting Alkemade-Keuls fonds, CHDR, ABBVIE, Hoffman-La Roche and OccamzRazor. W.D.J.v.d.B. received funding for a public–private partnership 'CONCERT' and 'ADAPT-PD' from Health~Holland, Topsector Life Sciences & Health in collaboration with Roche and Genentech. W.D.J.v.d.B. performed contract research for Roche Tissue Diagnostics, Discoveric Bio, AC Immune and Gain Therapeutics. All funding has been paid to Amsterdam UMC. W.D.J.v.d.B. is a member of the scientific advisory board of Gain Therapeutics and Alzheimer Nederland. W.D.J.v.d.B. is the president of the Dutch association for Parkinson Scientists and member of the board of the Parkinsonalliance Netherlands. As of 01 Nov 2025, E.A.J.W. is a contractor for Roche Diagnostics International. C.E.T. has research contracts with Acumen, ADx Neurosciences, AC Immune, Alamar, Aribio, Axon Neurosciences, Beckman Coulter, BioConnect, Bioorchestra, Brainstorm Therapeutics, C2N diagnostics, Celgene, Cognition Therapeutics, EIP Pharma, Eisai, Eli Lilly, Fujirebio, Instant Nano Biosensors, Merck, Muna, Nitrase Therapeutics, Novo Nordisk, Olink, PeopleBio, Quanterix, Roche, Sysmex, Toyama, Vaccinex and Vivoryon. C.E.T. is editor-in-chief of Alzheimer Research and Therapy, serves on the editorial boards of Molecular Neurodegeneration, Alzheimer's & Dementia, Neurology: Neuroimmunology & Neuroinflammation, and MedidactNeurologie/Springer, and is a member of the committee to define guidelines for cognitive disturbances and a committee for acute neurology in the Netherlands. C.E.T. has contracts with Aribio, Biogen, Beckman Coulter, Cognition Therapeutics, Danaher, Eisai, Eli Lilly, Janssen, Merck, Neurogen Biomarking, Nordic Biosciences, Novo Nordisk, Novartis, Olink, Quanterix, Roche, Sanofi and Veravas. The other authors declare no competing interests.

Additional information

Extended data is available for this paper at https://doi.org/10.1038/s41591-026-04212-0.

Supplementary information The online version contains supplementary material available at https://doi.org/10.1038/s41591-026-04212-0.

Correspondence and requests for materials should be addressed to Katharina Bolsewig.

Peer review information *Nature Medicine* thanks Mohamed Salama and the other, anonymous, reviewer(s) for their contribution to the peer review of this work. Primary Handling Editor: Jerome Staal, in collaboration with the *Nature Medicine* team.

https://doi.org/10.1038/s41591-026-04212-0

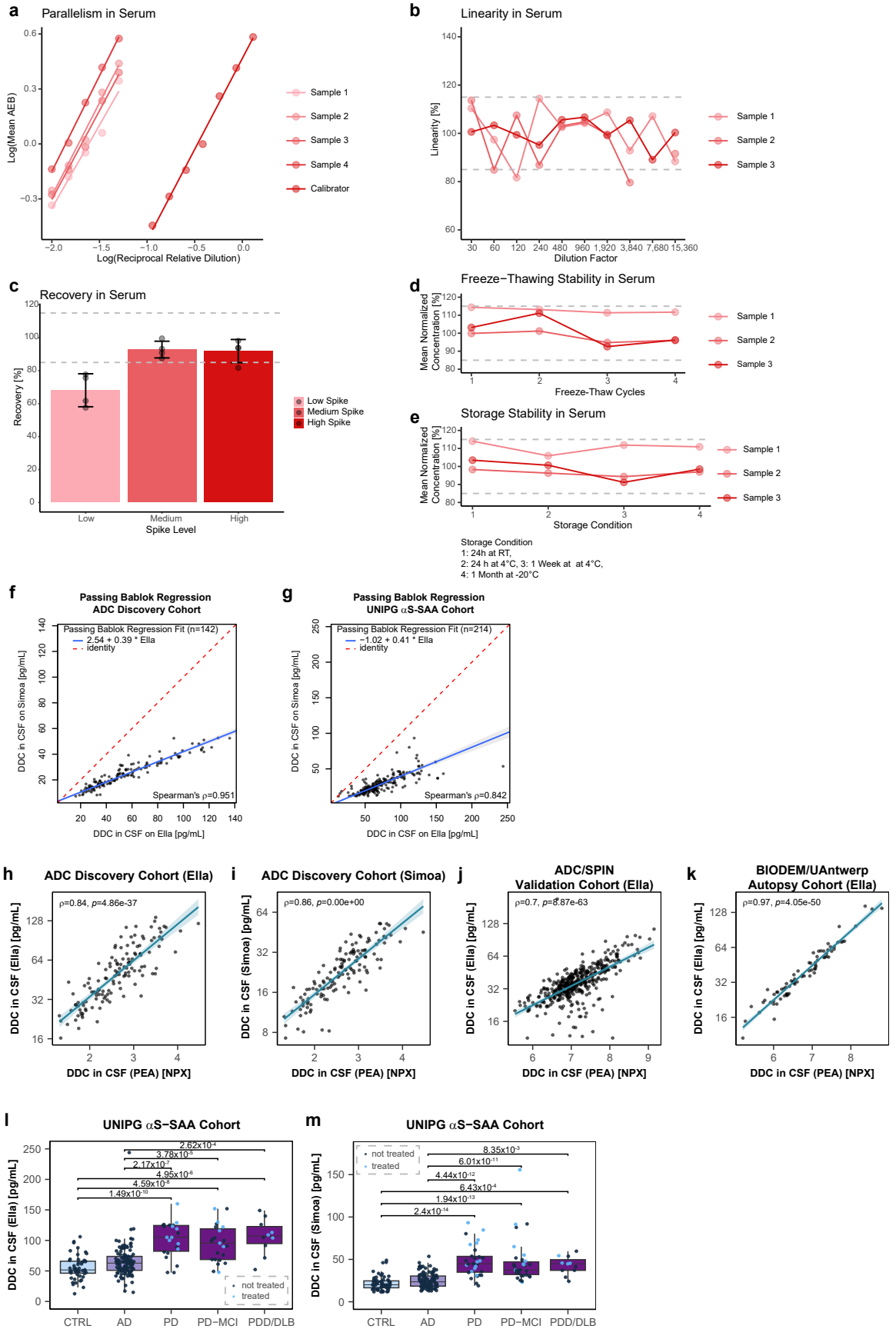

Extended Data Fig. 1 | See next page for caption.

https://doi.org/10.1038/s41591-026-04212-0

Extended Data Fig. 1 | Analytical validation results of Simoa assay in CSF, inter-method correlations and CSF DDC levels across different LBD subgroups. Visual presentation of analytical validation results of the in-house developed Simoa serum assay for the parameters parallelism (**a**), dilution linearity (**b**), recovery (**c**), freeze-thawing stability (**d**) and storage stability (**e**). Mean recovery and corresponding standard deviation (error bars in **c**) were calculated based on 4 individual serum samples. For all parameters, a range of 85% to 115% compared to the reference condition was accepted. In-house developed immunoassays showed a strong, linear correlation allowing for transforming values across methods (**f**, **g**). Passing Bablok regression was used to generate transformation formulas between in-house developed immunoassays and is indicated by the blue line. The transparent areas represent the 95% confidence intervals around the mean estimated values of the regression model. DDC measurements on the in-house developed immunoassays correlated strongly with PEA measurements (**h**–**k**). Correlation between in-house developed immunoassays and PEA was assessed by two-sided Spearman's correlation. Dark lines represent regression lines and transparent areas represent 95% confidence intervals. Boxplots illustrate DDC levels across diagnostic groups in the UNIPG αS-SAA as measured with Ella (**l**) or Simoa (**m**). The PD + DLB group was separated into the included sub-diagnoses PD (n = 33), PD-MCI (n = 34), and PDD/DLB (n = 11). DDC differences between diagnostic groups were assessed by ANCOVA corrected for age and sex with two-sided post-hoc Tukey's test and Bonferroni correction. Boxplots show DDC levels across diagnostic groups. Lines through the boxes indicate the median value and lower and upper lines correspond to the first and third quartiles. Dots represent individual data points and whiskers extend to 1.5 times of the interquartile range. Abbreviations: AD, Alzheimer's disease dementia; AEB, Average number of enzymes per bead; CTRL, Controls; DDC, DOPA Decarboxylase; DLB, Dementia with Lewy bodies; MCI, Mild cognitive impairment; NPX, Normalized Protein Expression; PD, Parkinson's disease; PDD, Parkinson's disease dementia; PEA, Proximity extension array; RT, Room temperature.

https://doi.org/10.1038/s41591-026-04212-0

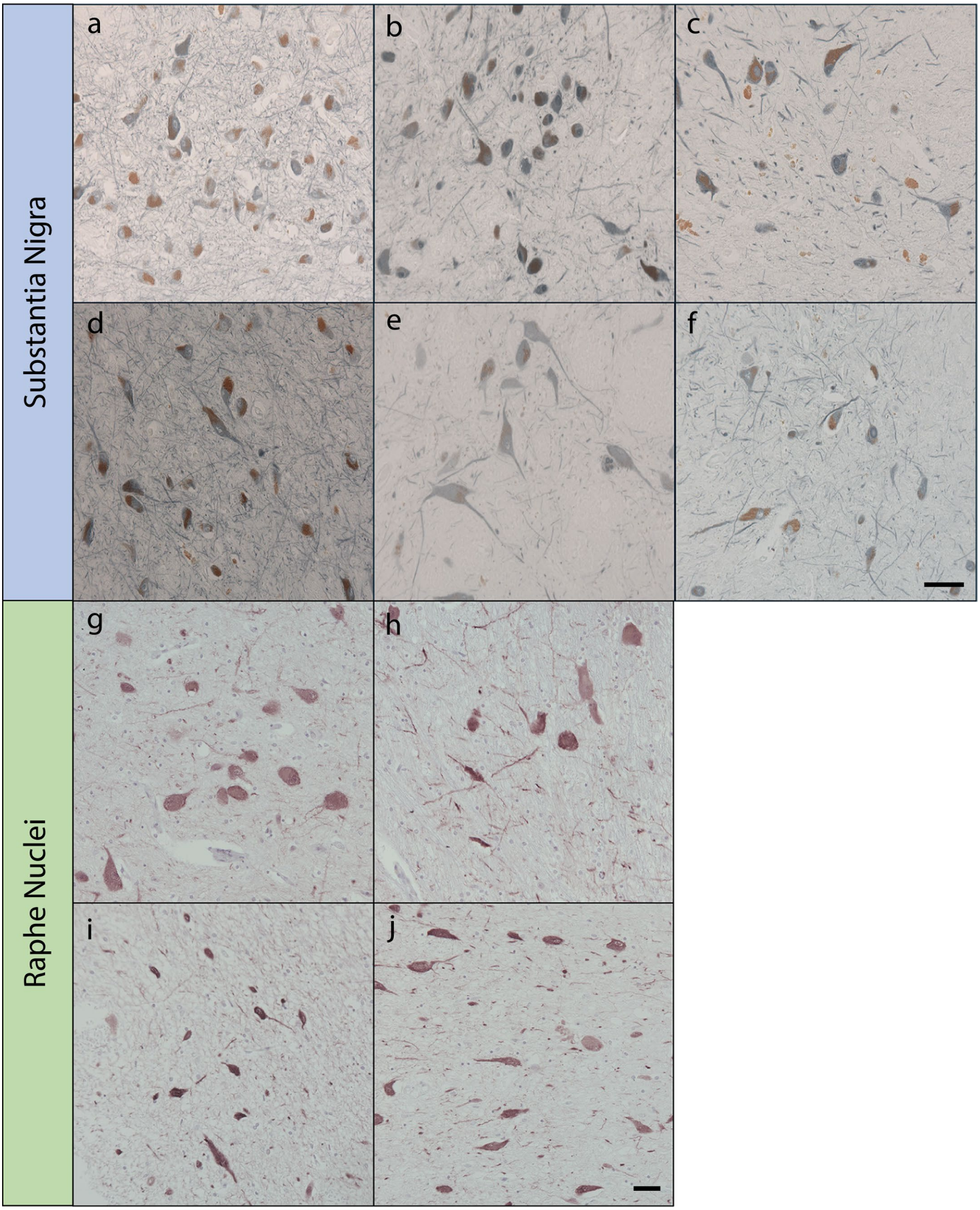

Extended Data Fig. 2 | See next page for caption.

https://doi.org/10.1038/s41591-026-04212-0

Extended Data Fig. 2 | Immunohistochemical stainings in post-mortem substantia nigra and raphe nuclei tissue. DDC (grey) was detected in the nucleus, soma and processes of dopaminergic neurons (neuromelanin in brown) in SN tissue from control (**a**, **d**), DLB (**b**, **e**) and PD(D) donors (**c**, **f**). Overall, more cells were detected in control tissue, but DDC reactivity was strongly observed in DLB and PD(D) tissue. DDC (red) was detected in serotonergic neurons in the raphe nuclei in brain tissue from controls (female, 73 years **g**, **h**; male, 49 years, **i**) and from a patient with PD (male, 76 years, **j**). Stainings were performed in post-mortem brain tissue from neurologically healthy controls (n = 4), patients with DLB (n = 4) and patients with PD(D) (n = 4; Extended Data Table 8). Stainings in post-mortem raphe nuclei tissue were performed according to Supplementary Methods 5. Representative pictures were taken from individual brain donors. Bars **a**–**f** = 50 µm and **g**–**j** = 50 µm.

https://doi.org/10.1038/s41591-026-04212-0

Extended Data Table 1 | Demographic characteristics of the clinically-defined fluid study cohorts

ADC Discovery Cohort	CTRL	DLB	AD		*p*
n	50	41	51		
Sex, Female (%)	24 (48.0)	3 (7.3)	26 (52.0)		2.92E-06
Age, years (median [IQR])	61.0 [58.0, 64.0]	70.5 [64.5, 74.8]	68.0 [62.8, 72.0]		1.90E-07
MMSE (mean (SD))	28.4 (1.2)	22.4 (4.1)	17.2 (5.2)		2.28E-13
Aβ42, pg/mL (mean (SD))[a)]	1159.5 (175.1)	817.1(239.8)	586.9 (103.2)		1.42E-32
pTau, pg/mL (mean (SD))[a)]	39.2 (10.8)	51.8 (20.6)	100.7 (50.9)		4.55E-16
tTau, pg/mL (mean (SD))[a)]	231.3 (79.3)	344.9 (143.5)	859.9 (462.2)		4.10E-20
DDC in CSF Ella, pg/mL (mean (SD))	39.47 (16.37)	84.66 (25.88)	45.37 (14.55)		2.45E-22
DDC in CSF Simoa, pg/mL (mean (SD))	18.19 (7.85)	35.98 (9.53)	21.40 (6.41)		3.43E-20
ADC/SPIN Validation Cohort	**CTRL**	**DLB**	**MCI-A+**	**AD**	***p***
n	108	106	101	104	
Sex, Female (%)	54 (50.0)	30 (28.3)	47 (46.5)	52 (50.0)	0.003
Age, years (median [IQR])	59.00 [56.00, 64.00]	73.00 [69.00, 78.00]	70.00 [67.00, 73.00]	69.00 [63.00, 74.00]	4.05E-36
MMSE (mean (SD))	28.79 (1.20)	22.56 (4.16)	25.82 (2.59)	20.81 (3.73)	1.64E-60
MoCA (mean (SD))[b)]	25.35 (2.18)	19.34 (4.19)	23.00 (2.83)	13.00 (NA)	8.00E-09
Aβ42 (ADC), pg/mL;	ADC: 1670.71 (347.57)	ADC: 955.22 (456.89)	ADC: 789.22 (225.58)	ADC: 683.65 (180.35)	ADC: 1.03e-39
Aβ42/40 (SPIN) (mean (SD))[c)]	SPIN: 0.1 (0.01)	SPIN: 0.07 (0.03)	SPIN: 0.04 (0.01)	SPIN: 0.04 (0.01)	SPIN: 8.37e-52
pTau, pg/mL (mean (SD))[c)]	ADC: 18.31 (8.18)	ADC: 19.34 (9.95)	ADC: 35.96 (14.87)	ADC: 31.08 (18.93)	ADC: 1.13e-11
	SPIN: 38.36 (11.89)	SPIN: 91.55 (70.65)	SPIN: 117.24 (58)	SPIN: 141.47 (75.95)	SPIN: 3.945e-16
tTau, pg/mL (mean (SD))[c)]	ADC: 196.05 (74.28)	ADC: 207.74 (83.07)	ADC: 326.19 (139.64)	ADC: 319.87 (186.44)	ADC: 6.08e-09
	SPIN: 262.09 (78.36)	SPIN: 572.09 (423.74)	SPIN: 714.38 (338.22)	SPIN: 874.86 (414.83)	SPIN: 1.091e-16
DDC in CSF Ella, pg/mL (mean (SD))	30.27 (7.97)	49.10 (18.81)	35.73 (11.10)	39.46 (20.89)	2.71E-16
DDBB/BMDB Validation Cohort	**CTRL**	**DLB**	**PD**	**AD**	***p***
n	42	47	37	52	
Sex, Female (%)	16 (38.1)	8 (17.0)	10 (27.0)	13 (25.0)	0.244
Age, years (median [IQR])	65.50 [55.00, 72.00]	74.00 [68.00, 77.50]	69.00 [62.00, 76.00]	72.50 [66.00, 77.25]	0.003
MMSE* (mean (SD))	28.29 (2.72)	24.71 (3.69)	24.44 (4.65)	23.56 (4.89)	5.68E-04
Aβ42, pg/mL* (mean (SD))[a)]	1143.54 (196.20)	756.78 (285.66)	785.23 (291.57)	487.52 (168.70)	1.96E-21
pTau, pg/mL* (mean (SD))[a)]	41.71 (9.71)	46.56 (22.29)	41.63 (24.76)	50.13 (38.34)	0.574
tTau, pg/mL* (mean (SD))[a)]	265.39 (66.72)	363.25 (192.94)	346.29 (292.52)	805.12 (221.11)	8.49E-24
DDC in CSF Simoa, pg/mL (mean (SD))	20.93 (7.01)	41.16 (13.62)	53.36 (35.96)	32.91 (11.85)	2.48E-10

P-values are based on χ2-Test to compare categorical variables, ANOVA to compare variable means and Kruskal-Wallis test to compare variable medians. All tests were two-sided. a) Measured by Innotest; b) MoCA was performed in a subset of participants from the ADC: CTRL=31, DLB=29, MCI-A+=2, AD=1; c) Measured by Innotest or Elecsys (ADC), and Lumipulse (SPIN). Innotest measurements were transformed to Elecsys measurements according to previously published conversion formulas[13]. Abbreviations: AD, Alzheimer's disease dementia; CTRL, Controls; DDC, DOPA Decarboxylase; DLB, Dementia with Lewy bodies; MCI, Mild cognitive impairment; MMSE, Mini mental stage examination; PD, Parkinson's disease.

https://doi.org/10.1038/s41591-026-04212-0

Extended Data Table 2 | Demographic characteristics of biologically- and pathologically-confirmed fluid study cohorts

UNIPG α-SAA Cohort*	CTRL	PD+DLB	AD	*p*
n	65	78	110	
Sex, Female (%)	31 (47.7)	28 (35.9)	74 (67.3)	7.99E-05
Age, years (median [IQR])	70.0 [63.0, 75.0]	66.0 [62.2, 71.8]	73.0 [70.0, 76.0]	3.88E-07
MMSE/MoCA (mean (SD))[a)]	26.57 (2.99)	21.88(5.17)	21.01 (5.8)	3.07E-10
Aβ42/40 (mean (SD))b)	0.11 (0.02)	0.10 (0.03)	0.05 (0.01)	2.57E-56
pTau, pg/mL (mean (SD))b)	36.26 (9.44)	41.81 (20.28)	114.63 (60.73)	8.23E-33
tTau, pg/mL (mean (SD))b)	265.43(140.74)	282.28 (178.8)	810.01 (393.85)	1.56E-34
αS-SAA positivity (%)	0 (0.0)	78 (100.0)	56 (50.9)	9.06E-46
DDC in CSF Ella, pg/mL (mean (SD))[c)]	55.7 (19.1)	99.6 (29.4)	65.7 (25.8)	1.97E-17
DDC in CSF Simoa, pg/mL (mean (SD))[d)]	21.9 (8.3)	46.4 (21.3)	25.0 (8.5)	6.27E-25
DDC in plasma Simoa, pg/mL (mean (SD))[e)]	2181.3 (1665.9)	2592.2 (1641.0)	1426.3 (552.7)	0.009
BIODEM/UAntwerp Autopsy Cohort	**CTRL**	**DLB**	**AD**	***p***
n	30	18	30	
Sex, Female (%)	13 (43.3)	3 (16.7)	15 (50.0)	0.068
Age, years (median [IQR])	64.0 [61.2, 65.8]	75.5 [71.0, 81.0]	71.5 [64.0, 75.8]	3.66E-06
Aβ42, pg/mL (mean (SD))[f)]	1099.2 (201.9)	554.2 (256.3)	436.6 (206.6)	3.53E-17
pTau, pg/mL (mean (SD))[f)]	49.2 (15.4)	62.1 (37.5)	78.9 (48.5)	0.01
tTau, pg/mL (mean (SD))[f)]	231.9 (94.2)	507.7 (405.1)	587.0 (300.2)	1.06E-05
DDC in CSF Ella, pg/mL (mean (SD))	32.71 (13.54)	73.01 (31.21)	41.46 (23.76)	2.68E-07

P-values are based on χ2-Test to compare categorical variables, ANOVA to compare variable means and Kruskal-Wallis test to compare variable medians. All tests were two-sided. * In CSF, DDC was measured using both the Ella (n=216) and Simoa (n=245) immunoassays. Of these, 214 CSF samples were analyzed using both assays. In plasma, measurements were conducted exclusively with Simoa (n=92). Paired CSF and plasma measurements were available for 88 individuals. a) MMSE was available for CTRL n=48 and AD n=108; MoCA was available for PD+DLB n=70. b) Measured by Elecsys. c) CTRL n=51, PD+DLB n=55 (drug naïve n=36, treated =19), AD n=110. d)CTRL n=60, PD+DLB n=75 (drug naïve n=48, treated n=27), AD n=110. e) CTRL n=18, PD+DLB n=52 (drug naïve n=32, treated n=20), AD n=22f) Measured by Innotest. Abbreviations: AD, Alzheimer's disease dementia; CTRL, Controls; DDC, DOPA Decarboxylase; DLB, Dementia with Lewy bodies; MMSE, Mini mental stage examination; MoCA, Montreal Cognitive Assessment; PD, Parkinson's disease; αS-SAA, α-synuclein Seed-amplification assay.

https://doi.org/10.1038/s41591-026-04212-0

Extended Data Table 3 | Demographic characteristics of the DaT PET-defined fluid study cohort

YUHS DaT PET Cohort	Overall	DaT PET normal	DaT PET abnormal	*p*
n	102	24	78	
Age, years (median [IQR])	77.406 [70.026, 81.983]	71.025 [63.815, 77.919]	78.621 [73.099, 82.603]	0.003
Sex, Female (%)	49 (48.0)	19 (79.2)	30 (38.5)	0.001
MMSE (mean (SD))	21.552 (4.969)	21.667 (5.615)	21.515 (4.792)	0.904
Aβ42, pg/mL (mean (SD))	544.294 (359.205)	600.750 (383.541)	526.923 (352.145)	0.381
pTau, pg/mL (mean (SD))	15.099 (7.696)	14.248 (7.565)	15.362 (7.765)	0.538
pTau/Aβ42 ratio (mean (SD))	0.036 (0.026)	0.034 (0.027)	0.037 (0.027)	0.574
DDC in CSF Simoa, pg/mL (mean (SD))	51.311 (30.928)	51.837 (21.463)	51.150 (33.421)	0.925
αS-SAA abnormality, n(%)	48 (47.1)	10 (41.7)	38 (48.7)	0.642
DaT PET abnormality, n (%)	78 (76.5)	0 (0.0)	78 (100.0)	7.31E-24
Presence of diagnosis [a)]				
DLB, n (%)	41 (40.2)	5 (20.8)	36 (46.2)	0.033
AD, n (%)	50 (49.0)	12 (50.0)	38 (48.7)	1
pLBD, n (%)	56 (54.9)	17 (70.8)	39 (50.0)	0.101
NPH, n (%)	55 (53.9)	8 (33.3)	47 (60.3)	0.034
VCI, n (%)	20 (19.6)	7 (29.2)	13 (16.7)	0.238
PSP, n (%)	3 (2.9)	0 (0.0)	3 (3.8)	1
svPPA, n (%)	1 (1.0)	1 (4.2)	0 (0.0)	0.235

P-values are based on χ2-Test to compare categorical variables, ANOVA to compare variable means and Kruskal-Wallis test to compare variable medians. All tests were two-sided. Abbreviations: AD, Alzheimer's disease; CSF, Cerebrospinal fluid; DaT, Dopamine transporter; DDC, DOPA Decarboxylase; DLB, Dementia with Lewy bodies; MMSE, Mini-Mental State Examination; NPH, normal pressure hydrocephalus; PET, positron emission tomography; pLBD, possible Lewy body disease; PSP, progressive supranuclear palsy; αS-SAA, α-synuclein seed amplification assay; svPPA, semantic variant primary progressive aphasia; VCI, vascular cognitive impairment. a) One or more etiologies for cognitive impairment were decided based on clinical history, neurological examination, CSF AD biomarkers and brain magnetic resonance imaging.

https://doi.org/10.1038/s41591-026-04212-0

Extended Data Table 4 | ANCOVA group comparison estimated and significance parameters

Cohort	Group comparison	*β* (95% CI)	Fold-change	*p* -value
ADC Discovery Cohort (CSF, Ella)	DLB vs CTRL	0.33 (0.24 to 0.43)	2.2	1.61E-14
	DLB vs AD	0.27 (0.19 to 0.36)	1.9	1.80E-12
ADC Discovery Cohort (CSF, Simoa)	DLB vs CTRL	0.31 (0.22 to 0.40)	2	1.65E-13
	DLB vs AD	0.23 (0.15 to 0.31)	1.7	1.51E-09
ADC/SPIN Validation Cohort (CSF, Ella)	DLB vs CTRL	0.14 (0.07 to 0.21)	1.6	9.89E-07
	DLB vs MCI-A+	0.11 (0.06 to 0.16)	1.4	2.74E-06
	DLB vs AD	0.08 (0.03 to 0.13)	1.2	0.001
	AD vs CTRL	0.06 (0.0005 to 0.12)	1.3	0.048
DDBB/BMDB Validation Cohort (CSF, Simoa)	DLB vs CTRL	0.25(0.16 to 0.34)	2	1.65E-10
	DLB vs AD	0.09 (0.01 to 0.18)	1.3	0.02
	PD vs CTRL	0.35 (0.26 to 0.44)	2.5	1.11E-16
	PD vs AD	0.19 (0.10 to 0.29)	1.6	4.47E-07
	PD vs DLB	0.10 (0.008 to 0.19)	1.3	0.026
	AD vs CTRL	0.16 (0.07 to 0.24)	1.6	6.60E-05
UNIPG αS-SAA Cohort (CSF, Ella)	PD+DLB vs CTRL	0.26 (0.19 to 0.33)	1.8	4.88E-15
	PD+DLB vs AD	0.19 (0.12 to 0.26)	1.5	2.36E-10
	AD vs CTRL	0.07 (0.005 to 0.13)	1.2	0.03
	PD+DLB (DN) vs CTRL	0.23 (0.14 to 0.33)	1.7	6.39E-10
	PD+DLB (DN) vs AD	0.16 (0.08 to 0.24)	1.5	2.32E-10
	PD+DLB (T) vs CTRL	0.31 (0.20 to 0.43)	2	1.30E-11
	PD+DLB (T) vs AD	0.24 (0.14 to0.35)	1.7	3.71E-08
	PD+DLB (T) vs PD+DLB (DN)	0.08 (-0.04 to 0.20)	1.2	0.32
UNIPG αS-SAA Cohort (CSF, Simoa)	PD+DLB vs CTRL	0.31 (0.25 to 0.37)	2.1	0.00E+00
	PD+DLB vs AD	0.24 (0.18 to 0.30)	1.9	0.00E+00
	AD vs CTRL	0.07 (0.01 to 0.13)	1.1	0.014
	PD+DLB (DN) vs CTRL	0.27 (0.19 to 0.35)	1.9	0.00E+00
	PD+DLB (DN) vs AD	0.20 (0.13 to 0.27)	1.6	6.46E-12
	PD+DLB (T) vs CTRL	0.39 (0.29 to 0.48)	2.5	0.00E+00
	PD+DLB (T) vs AD	0.32 (0.23 to 0.40)	1.9	0.00E+00
	PD+DLB (T) vs PD+DLB (DN)	0.12 (0.02 to 0.21)	1.4	9.71E-03
UNIPG αS-SAA Cohort (Plasma, Simoa)	PD+DLB vs CTRL	0.06 (-0.11 to 0.23)	1.2	0.663
	PD+DLB vs AD	0.17 (-0.001 to 0.34)	1.8	0.052
	PD+DLB (DN) vs CTRL	-0.02 (-0.22 to 0.18)	0.9	0.998
	PD+DLB (DN) vs AD	0.09 (-0.1 to 0.28)	1.1	0.618
	PD+DLB (T) vs CTRL	0.21 (-0.02 to 0.43)	1.6	0.089
	PD+DLB (T) vs AD	0.31 (0.10 to 0.52)	2.5	1.10E-03
	PD+DLB (T) vs PD+DLB (DN)	0.22 (0.04 to 0.42)	1.8	0.011
BIODEM/UAntwerp Autopsy Cohort (CSF, Ella)	DLB vs CTRL	0.31 (0.15 to 0.48)	2.2	6.06E-05
	DLB vs AD	0.25 (0.10 to 0.39)	1.8	3.33E-04

DDC differences between diagnostic groups were assessed across groups by ANCOVA corrected for age and sex with two-sided post-hoc Tukey's test and Bonferroni correction.
Abbreviations: AD, Alzheimer's disease; CI, confidence interval; DLB, dementia with Lewy bodies; CTRL, Controls; PD, Parkinson's disease; S, α-synuclein seed-amplification assay status.

https://doi.org/10.1038/s41591-026-04212-0

Extended Data Table 5 | ROC analysis with models DDC only and basic models

Cohort		DDC only model				Basic model		
		AUC	Threshold / Cut-off	Spec.	Sens.	AUC	Spec.	Sens.
ADC Discovery Cohort (Ella)	DLB vs HC	0.926	54.1	0.86	0.9	0.873	0.82	0.78
	DLB vs AD	0.904	60.4	0.86	0.83	0.769	0.51	0.98
ADC Discovery Cohort (Simoa)	DLB vs HC	0.914	27.1	0.88	0.88	0.873	0.82	0.78
	DLB vs AD	0.899	27.7	0.84	0.88	0.769	0.51	0.98
ADC/SPIN Validation Cohort (Ella)	DLB vs HC	0.835	38.9	0.86	0.69	0.942	0.86	0.9
	DLB vs MCI-A+	0.733	40.7	0.79	0.66	0.682	0.9	0.37
	DLB vs AD	0.682	40.8	0.68	0.66	0.726	0.79	0.58
DDBB/BMDB Validation Cohort (Simoa)	DLB vs HC	0.927	31.1	0.95	0.72	0.725	0.74	0.64
	DLB vs AD	0.691	30.1	0.58	0.77	0.562	0.46	0.74
	PD vs HC	0.94	31.5	0.95	0.87	0.6	0.24	0.97
	PD vs AD	0.778	30.3	0.6	0.89	0.612	0.88	0.32
UNIPG αS-SAA Cohort (Ella)	PD+DLB vs HC	0.885	67.4	0.8	0.85	0.608	0.39	0.84
	PD+DLB vs AD	0.827	78.7	0.8	0.75	0.781	0.64	0.84
	PD+DLB (DN) vs HC	0.854	67.4	0.8	0.81	0.59	0.39	0.86
	PD+DLB (DN) vs AD	0.778	78.7	0.8	0.64	0.771	0.64	0.86
	PD+DLB (T) vs HC	0.945	84.5	0.92	0.95	0.643	0.24	1
	PD+DLB (T) vs AD	0.92	89.5	0.88	0.89	0.8	0.46	1
UNIPG αS-SAA Cohort (Simoa)	PD+DLB vs HC	0.926	29.4	0.87	0.88	0.581	0.35	0.84
	PD+DLB vs AD	0.886	29	0.72	0.89	0.781	0.59	0.85
	PD+DLB (DN) vs HC	0.909	26.8	0.82	0.9	0.575	0.35	0.85
	PD+DLB (DN) vs AD	0.852	29	0.72	0.85	0.774	0.59	0.85
	PD+DLB (T) vs HC	0.957	34.5	0.93	0.93	0.591	0.38	0.81
	PD+DLB (T) vs AD	0.946	35.5	0.88	0.93	0.794	0.72	0.74
BIODEM/ UAntwerp Autopsy Cohort (Ella)	DLB vs HC	0.927	45.5	0.87	0.89	0.977	1	0.83
	DLB vs AD	0.844	47.3	1	1	0.745	0.73	0.72

https://doi.org/10.1038/s41591-026-04212-0

Extended Data Table 6 | Status of clinical core features and DaT scan in ADC and SPIN Cohorts

	ADC Discovery Cohort	ADC/SPIN Validation Cohort
	DLB	DLB
n	42	106
Parkinsonism (n present/n not present/NA)	5-3-1934	70/11/25
Fluctuations (n present/n not present/NA)	4-4-1934	53/18/35
Hallucinations (n present/n not present/NA)	5-4-1933	48/31/27
RBD (n present/n not present/NA)	5-3-1934	42/32/32
DaT scan (n abnormal/n normal/NA)	5-1-1936	38/10/58

Abbreviations: DaT, Dopamine transporter; DLB, dementia with Lewy bodies; NA, data not assessed; RBD, REM sleep behavior disorder.

https://doi.org/10.1038/s41591-026-04212-0

Extended Data Table 7 | Association of CSF DDC concentrations with DaT uptake values

	Caudate			Putamen			Caudate/Putamen		
Diagnosis	β (SE)	p	q	β (SE)	p	q	β (SE)	p	q
All participants	-0.315 (0.303)	0.301	0.452	0.031 (0.330)	0.926	0.926	-0.097 (0.054)	0.073	0.219
Drug- naïve participants	-0.389 (0.413)	0.35	0.443	0.329 (0.425)	0.443	0.443	-0.201 (0.060)	0.0015	0.0045

Data are results of two-sided general linear models for DaT uptake values using CSF DDC as a predictor after controlling for age, sex, and education. Q-values were adjusted for multiple testing by Benjamini-Hochberg correction.

https://doi.org/10.1038/s41591-026-04212-0

Extended Data Table 8 | Demographics and neuropathological features of the immunohistochemistry study cohort

	Control	DLB	PD(D)
n	4	4	4
Sex, F (%)	2 (50%)	1 (25%)	1 (25%)
Age at death, years (median [IQR])	81 (8.2)	81 (5.2)	73.5 (4.7)
Disease duration, months or years (mean (SD))	NA	3.5 (1.3)	19.75 (7.6)
PMD, hh:mm (mean (SD))	06:57 (00:29)	04:36 (00:32)	06:55 (01:03)
Braak NFT stage (0-6; range)	1-3	1-3	1-2
Braak αSyn stage (0-6; range)	0	6	6
Thal Phase (0-5; range)	0-2	2-3	1-3

Abbreviations: αSyn, alpha-synuclein; ABC, amyloid, Braak, CERAD ((Consortium to Establish a Registry for Alzheimer's Disease); DLB, dementia with Lewy bodies; hh, hours; mm, minutes; NFT, neurofibrillary tangle; PD(D), Parkinson's disease (dementia); PMD, post-mortem delay.

nature portfolio

Corresponding author(s): Katharina Bolsewig

Last updated by author(s): Nov 25, 2025

Reporting Summary

Nature Portfolio wishes to improve the reproducibility of the work that we publish. This form provides structure for consistency and transparency in reporting. For further information on Nature Portfolio policies, see our Editorial Policies and the Editorial Policy Checklist.

Statistics

For all statistical analyses, confirm that the following items are present in the figure legend, table legend, main text, or Methods section.

n/a	Confirmed
☐	☒ The exact sample size (*n*) for each experimental group/condition, given as a discrete number and unit of measurement
☐	☒ A statement on whether measurements were taken from distinct samples or whether the same sample was measured repeatedly
☐	☒ The statistical test(s) used AND whether they are one- or two-sided *Only common tests should be described solely by name; describe more complex techniques in the Methods section.*
☐	☒ A description of all covariates tested
☐	☒ A description of any assumptions or corrections, such as tests of normality and adjustment for multiple comparisons
☐	☒ A full description of the statistical parameters including central tendency (e.g. means) or other basic estimates (e.g. regression coefficient) AND variation (e.g. standard deviation) or associated estimates of uncertainty (e.g. confidence intervals)
☐	☒ For null hypothesis testing, the test statistic (e.g. *F*, *t*, *r*) with confidence intervals, effect sizes, degrees of freedom and *P* value noted *Give P values as exact values whenever suitable.*
☒	☐ For Bayesian analysis, information on the choice of priors and Markov chain Monte Carlo settings
☒	☐ For hierarchical and complex designs, identification of the appropriate level for tests and full reporting of outcomes
☒	☐ Estimates of effect sizes (e.g. Cohen's *d*, Pearson's *r*), indicating how they were calculated

Our web collection on statistics for biologists contains articles on many of the points above.

Software and code

Policy information about availability of computer code

Data collection	No custom code has been developed for this study.
Data analysis	All statistical analyses were performed using R (version 4.0.3), as described in the manuscript section "Statistics & Reproducibility".

For manuscripts utilizing custom algorithms or software that are central to the research but not yet described in published literature, software must be made available to editors and reviewers. We strongly encourage code deposition in a community repository (e.g. GitHub). See the Nature Portfolio guidelines for submitting code & software for further information.

Data

Policy information about availability of data

All manuscripts must include a data availability statement. This statement should provide the following information, where applicable:

- Accession codes, unique identifiers, or web links for publicly available datasets
- A description of any restrictions on data availability
- For clinical datasets or third party data, please ensure that the statement adheres to our policy

Data access to anonymized patient-level data from the study cohorts can be requested from the corresponding author on reasonable request and will be made available in accordance with the respective cohort PI. Anonymized data for each figure are made available in the source data file.

Research involving human participants, their data, or biological material

Policy information about studies with human participants or human data. See also policy information about sex, gender (identity/presentation), and sexual orientation and race, ethnicity and racism.

Reporting on sex and gender	Distribution of sex, based on self-reporting, did not differ significantly in the DDBB/BMDB and BIODEM/UAntwerp cohorts. Signficant differences in sex distribution were observed in the ADC Discovery Cohort (%female: CTRL=48.0, DLB=7.3, AD=52.0), ADC/SPIN Validation Cohort (%female: CTRL=50.0, DLB=28.3, MCI-A+=46.5, AD=50.0) and the αS-SAA UNIPG Cohort (%female: CTRL=47.7, PD+DLB=35.9, AD=67.3). Nevertheless, the inclusion of multiple cohorts lead to the inclusion of substantial numbers of female and male participants. Sex was included as a covariate in all statistical analyses, apart from regression analysis between paired plasma and CSF measurements and paired immunoassay and Olink proteomics measurements.
Reporting on race, ethnicity, or other socially relevant groupings	Albeit the reported impact of race and ethnicity on certain fluid biomarkers, we unfortunately did not have this information available for all cohorts. The far majority of participants from the ADC, SPIN, DDBB/BMDB, UNIPG and BIODEM/UAntwerp cohorts is white, while analyses of associations with DaT-PET were performed in asian participants. Overall, our study included too little diversity to study the effect of race/ethnicity in these cohorts.
Population characteristics	We observed significant differences of age between the diagnostic groups in all study cohorts. In the UNIPG Cohort, the PD +DLB group were overall younger (66.0 [62.2, 71.8] years) than the other diagnostic groups (CTRL: 70.0 [63.0, 75.0], AD: 73.0 [70.0, 76.0]), while in the other cohorts, controls were significantly younger than the patient groups. Age was included as a covariate in all statistical analyses, apart from regression analysis between paired plasma and CSF measurements and paired immunoassay and Olink proteomics measurements.
Recruitment	Recruitment of study participants is described in the mansucript section "Study population". Participants from the ADC Discovery Cohort were recruited from the Amsterdam Dementia Cohort and selected for the inclusion in a previous study (Del Campo et al., Nat Commun, 2023, DOI:10.1038/s41467-023-41122-y). Included controls were participants with subjective cognitive decline who did not present with any cognitive abnormalities during the diagnostic work-up. Participants from the ADC/SPIN Validation Cohort were recruited from the Amsterdam Dementia Cohort and the Sant Pau Initiative on Neurodegeneration study. Included controls were participants with subjective cognitive decline who did not present with any cognitive abnormalities during the diagnostic work-up, or volunteers with normal neuropsychological scores. Participants fromt he BIODEM/UAntwerp Autopsy Cohort were recruited from the Reference Center for Biological Markers of Dementia and the neurobiobank of the Institute Born-Bunge of the University of Antwerp. All participants with DLB and AD were pathologically confirmed at autopsy. Controls were not pathologically-confirmed and consisted of volunteers without any neurological or psychiatric diseases and did not present with any cognitive abnormalities. Participants from the DDBB/BMDB Validation Cohort were recruited from the Danish Dementia Biobank and Bispebjerg Movement Disorder Biobank. Controls were cognitively healthy individuals who were referred to diagnostic evaluation at the Danish Dementia Research Centre's memory clinic but who were found without dementia or MCI. Particiapnts from the UNIPG αS-SAA Cohort were recruited from the University of Perugia and selected based on available aS-SAA data. All participants in the PD+DLB group had an abnromal αS-SAA status. Controls were cognitively normal individuals or individuals with MCI who had a normal AD CSF biomarker profile and negative CSF αS-SAA. Participants from the YUHS DaT-PET Cohort were recruited from the Yonsei University Health System and were selected for available DaT-PET imaging. Participants were not compensated for participation in this study.
Ethics oversight	Informed written consent was given by all participants or their legal representatives, for their medical data and biomaterials to be used for scientific research. The study was conducted in accordance to the Declaration of Helsinki and was approved by the local ethical committees of each participating center (ADC: AD CSF biobank METC number 2017.315, SPIN: COLLECTION 16/2013, DDBB/BMDB Validation: H-23001553, UNIPG αS-SAA: Comitato Etico Aziende Sanitarie Regione Umbria 19369/AV and 20942/21/OV, BIODEM/UAntwerp Autopsy: EC of ZNA (Approval No 4363) and EC UZA/UAntwerp (14/12/130), YUHS DaT-PET: review board of Severance Hospital (IRB No. 4-2018-0944 and IRB No. 4-2024-0877).

Note that full information on the approval of the study protocol must also be provided in the manuscript.

Field-specific reporting

Please select the one below that is the best fit for your research. If you are not sure, read the appropriate sections before making your selection.

☒ Life sciences ☐ Behavioural & social sciences ☐ Ecological, evolutionary & environmental sciences

For a reference copy of the document with all sections, see nature.com/documents/nr-reporting-summary-flat.pdf

Life sciences study design

All studies must disclose on these points even when the disclosure is negative.

Sample size	We included all participants with available and quality control-passing DDC measurements (on Ella or Simoa platform).

Data exclusions	Participants were excluded from subanalyses when required cognitive or clinical data were missing.
Replication	We used six different independent cohorts to validate our findings. Findings were consistent across different cohorts, i.e. each attemp for replication was successful.
Randomization	Randomization does not apply as we did not perform any intervention.
Blinding	All operating staff was blinded to clinical data.

Reporting for specific materials, systems and methods

We require information from authors about some types of materials, experimental systems and methods used in many studies. Here, indicate whether each material, system or method listed is relevant to your study. If you are not sure if a list item applies to your research, read the appropriate section before selecting a response.

Materials & experimental systems

n/a	Involved in the study
☐	☒ Antibodies
☒	☐ Eukaryotic cell lines
☒	☐ Palaeontology and archaeology
☒	☐ Animals and other organisms
☒	☐ Clinical data
☒	☐ Dual use research of concern
☒	☐ Plants

Methods

n/a	Involved in the study
☒	☐ ChIP-seq
☒	☐ Flow cytometry
☒	☐ MRI-based neuroimaging

Antibodies

Antibodies used	anti DDC (R&D Sytems; MAB3564; Clone# 413911; capture), anti DDC (R&D Systems; BAF3564; detection), anti TH (Chemicon; MAB318; Clone# LNC1), anti p-syn (Abcam; ab51253; Clone# EP1536Y),
Validation	Anti DDC antibody (MAB3564; Clone# 413911; capture): Characterized by antibody vendor (R&D Systems; https://www.rndsystems.com/products/human-dopa-decarboxylase-ddc-antibody-413911_mab3564) through western blot and specificity has been assessed in DDC KO human cell models. Anti DDC antibody (BAF3564, detection; AF3564, IHC): Characterized by vendor (R&D Systems;https://www.rndsystems.com/products/human-dopa-decarboxylase-ddc-biotinylated-antibody_baf3564 and https://www.rndsystems.com/products/human-mouse-rat-dopa-decarboxylase-ddc-antibody_af3564) through western blot and IHC. Furthermore, the antibody was tested in western blot, mouse tissue and iPSC cells. anti TH (MAB318, Clone# LNC1, Chemicon): Has been characterized and validated by antibody vendor for use in IH, IH(P), IP and western blot. More than 85 citations reported the use of this antibody (e.g. DOI: 10.1007/s00429-019-01960-3). anti p-syn (ab51253, Clone# EP1536Y, Abcam): Characterized by antibody vendor thoprugh western blot in different matrices and IHC. Furthermore, the antibody is widely used to detect phosphorylated-synuclein (e.g. DOI: 10.1038/s41467-025-61052-1).

Plants

Seed stocks	NA
Novel plant genotypes	NA
Authentication	NA